SIMULATING THE EFFECTS OF CLIMATE CHANGE ON CLOUD FORMATIONS AROUND MOUNTAINOUS ISLANDS

A THESIS SUBMITTED TO
THE GLOBAL ENVIRONMENTAL SCIENCE
UNDERGRADUATE DIVISION IN PARTIAL FULFILLMENT
OF THE REQUIREMENTS FOR THE DEGREE OF

BACHELOR OF SCIENCE

IN

GLOBAL ENVIRONMENTAL SCIENCE

Spring 2021

By
Kayla White

Thesis Advisor

Dr. Giuseppe Torri

I certify that I have read this thesis and that, in my opinion, it is satisfactory in scope and quality as a thesis for the degree of Bachelor of Science in Global Environmental Science.

THESIS ADVISOR

Giuseppe Torri

Dr. Giuseppe Torri
Department of Atmospheric Sciences

For my family and friends who are always encouraging me to push my limits of learning.

ACKNOWLEDGEMENTS

I would like to thank my mentor, Dr. Giuseppe Torri, for guiding me through this thesis project and encouraging me to ask questions and push the limits of the model. I would like to thank the Global Environmental Science Program, including the department chair Dr. Michael Guidry, for the support in the completion of my project. I would like to thank my fellow SOEST classmates for the support with my undergraduate thesis because without collaboration, I feel I would have been lost. Lastly, I would like to thank my friends and family for encouraging me to take every advantage I could of my undergraduate degree and this thesis project.

ABSTRACT

If islands are large enough and far enough from other continents, they can act as developers for convection in the tropics due to their diurnal cycle (Sobel et al. 2001). In order to better understand what climate change might bring to the Maritime Continent and other tropical islands, like Hawai‘i, I simulated the effects of global warming by increasing the sea surface temperature surrounding a flat and mountainous island. Numerical simulations were run with a sea surface temperature spanning the range between 300K to 303K with 0.5K increments, and statistical analysis was run on each of these executables, looking at the mixing ratio of the water vapor, zonal, vertical, and meridional velocity, potential temperature, relative humidity, cloudiness, rainfall rate and surface temperature. After running statistical analysis with a control flat island of the same size, we added a mountain to the simulation and compared these results with the control island. Statistical analysis was run on the mountainous island for each sea surface temperature, looking at the same variables. We found that, as the sea surface temperature increased, precipitation and cloud formations over the flat and mountainous island were larger and more extreme due to the larger temperature contrast between the ocean and land. As climate change causes the sea surface temperature to warm, cloud formations and rainfall rate are expected to increase above and around islands.

TABLE OF CONTENTS

LIST OF TABLES

LIST OF FIGURES

1.0 INTRODUCTION

1.1 Background

Islands are key developers of convection in the tropics and, if they are large enough and far enough away from other continents, they can be seen as localized forcings in the middle of the ocean (Sobel et al. 2011). The forcing of these larger islands comes from the lower heat capacity of the land relative to the ocean surrounding the island. Land heats and cools faster than water, creating temperature differences between the land and ocean. This temperature difference leads to pressure differences above and around the island depending on the time of day which leads to a cyclical circulation pattern. The heating of these contrasted surfaces results in a sea breeze circulation in the day when the land heats up and wind blows the cooler air from the ocean towards the land. A smaller land breeze follows at night, pushing the cooler air on land back out to sea (Mori et al. 2004, Qian 2008). This land-sea breeze cycle controls the diurnal circulation of precipitation and convection over many tropical islands (Coppin and Bellon 2019). During the daytime of the diurnal cycle, clouds and precipitation are concentrated over the land, peaking in the early evening (Coppin and Bellon 2019). During the nighttime of the diurnal cycle, clouds and precipitation are concentrated over the sea, as the land breeze pushes the cooler air from the land back out, with a peak in the early morning (Coppin and Bellon 2019).

Tropical islands are some of the rainiest places in the world, but recent studies show that the amount of rainfall and precipitation patterns above can be dependent on the topography of the island (Cronin et al. 2015). According to a study by Cronin et al.

(2014), small islands tend to be rainier than the nearby oceans and this contrast between land and water can increase with island size and elevation. More rain falls on small mountainous islands than small flat islands, but elevation and rainfall rate do not correlate when it comes to larger islands in the Maritime Continent (Dayem et al. 2007; As-syakur et al. 2013; Cronin et al. 2015). The descent of air in the Maritime Continent plays a large role in the general circulation of the atmosphere and most climate models do not have enough resolution to simulate the land-ocean precipitation contrast in detail (Cronin et al. 2015). Furthermore, the timing of the diurnal cycle of convective rainfall over tropical mountainous islands is poorly represented by climate models (Cronin et al. 2015). Attempting to connect these processes has led to hypotheses about the diurnal cycle of tropical islands that could be important in understanding convective intensity or the time of day precipitation peaks over small islands in the Maritime Continent, which may also be missing from climate models (Cronin et al. 2015). Moreover, the mechanisms that drive diurnal convection remain unclear and can vary, which is why the drivers are hard to capture in atmospheric models (Cronin et al. 2015). In many cases, tropical islands are completely reliant on the local rainfall as a source of freshwater. Understanding what brings rain to islands in the Maritime Continent and what might happen in the future is very important to help us understand issues related to water security and habitability.

Understanding the diurnal cycle of convection over the Maritime Continent is also important from an atmospheric circulation perspective. The Madden-Julian Oscillation (MJO) is an eastward-moving disturbance of winds, rainfall, clouds, and pressure that moves from the Indian Ocean to the Western Pacific, and it is one of the most important atmospheric phenomena on the planet (Peatman et al. 2014). There can be multiple MJO

events per season, so it can be described as intraseasonal climate variability. Due to the Maritime Continent's diverse topography, the nature of the MJO passing through this region is poorly understood (Peatman et al. 2014). Climate model simulations of the MJO are not well represented, leading to local errors in latent heat release and weather prediction errors on a much larger, global scale (Peatman et al. 2014). Furthermore, in the Maritime Continent, 80% of the MJO precipitation is affected by changes in the diurnal cycle (Peatman et al. 2014). Therefore, the Maritime Continent is a very important region to explore when it comes to climate and atmospheric models.

On the contrary, the understanding of the island diurnal cycle is limited since there are so many factors influencing the processes (Wang and Sobel 2017). Topography, wind, land-sea breezes, surface roughness, latitude, island size, and the contrasting temperatures between the land and sea can affect the diurnal cycle (Wang and Sobel 2017). Topography and the roughness of the island act as mechanical forcings for horizontal winds which have no diurnal cycle, whereas the thermal forcing of the island from surface heating driven by solar radiation should be diurnal (Wang and Sobel 2017). Expanding on this idea, studies from Sobel et. al (2011) showed that small islands in the Maritime Continent have stronger diurnal cycles during the low-wind season than small islands in the high wind season in the Caribbean (Wang and Sobel 2017).

Islands in the Maritime Continent can create perturbations to the lower atmospheric region, presenting a chance for understanding deep convection in these latitudes (Wang and Sobel 2017). Due to the close relationship between latent heating and upward tropical motion, Sobel et al. (2001) hypothesized that this implies the time-mean upward motion in the Maritime Continent is driven by rainfall enhancement.

Therefore, this mechanism changes what we might know about Walker Circulation (Dayum et al. 2007).

As shown by Neale and Slingo (2003) and Qian (2008), climate models disagree on the influence of land-ocean contrasts on rainfall on islands in the Maritime Continent. Neal and Slingo (2003) found that the regional precipitation biases were not reduced, even with a three-fold increase of resolution, but when they replaced land with ocean, the simulation improved locally and remotely (Cronin et al. 2015). On the contrary, Qian (2008) model of Java with parameterized convection found that realistic topography correctly reflected mean rainfall and its diurnal cycle, but found that, when flattening the island or replacing the land with ocean, it resulted in very low precipitation rates (Cronin et al. 2015). These varying rainfall responses in studies of Neale and Slingo (2003) and Qian (2008) show that the initial island rainfall enhancement mechanisms must also vary between different climate models. Another study by Robinson et al. (2008) showed that oscillating sensible heat flux diurnally could produce a resonance for islands of a certain size, leading to increased convective intensity locally. Nevertheless, the climate models from Neal and Slingo (2003), Qian (2008), and Robinson et al. (2008) stress the importance of dynamical convective forcings due to the convergence of land-sea and mountain-valley breezes (Cronin et al. 2015).

1.2 Main Analysis

Over a wide range of time scales, precipitation in the tropics varies greatly. But, due to its ability to modulate the components of longer scale phenomena, diurnal cycles can arguably be one of the most dominant sources of variability (Yokoi et al. 2017).

Since clouds only reflect solar radiation during the day, the diurnal cycle has considerable impacts on the radiation budget of land (Yokoi et al. 2017). Because of this, understanding all the processes involved in the diurnal cycle of convection is important in climate science and modelling islands in the Maritime Continent (Yokoi et al. 2017).

A study by Mori et al. (2004) showed that on the Western coast of Sumatra, precipitation tended to peak in the early evening and migrate offshore in the nighttime, almost 400 km out from the coast by the morning (Yokoi et al. 2017). The diurnal cycle over land is typically a direct response from the diurnal cycle of insulation whereas mechanisms for nighttime offshore diurnal cycles are not as well known (Yokoi et al. 2017).

We are interested in exploring the diurnal cycle of tropical islands using numerical models. This allows us to study processes above and around a tropical island in great detail thanks to idealized studies. In order to do this, we simulated a flat and a mountainous island. With each island, we varied the sea surface temperature (SST) to observe the effects on cloud formations and precipitation above and around each island. This study can provide insight into what might happen with a future of climate change and help fill in the gaps of what we know about diurnal cycles in the Maritime Continent.

1.3 Objective of Study

This study can help predict what global warming could bring to the Maritime Continent and more specifically, mountainous islands in the Maritime Continent. With sea surface temperatures rising in many parts of the globe, interactions between the atmosphere and hydrosphere are changing, which could bring new, extreme weather

conditions.

Apart from those cited in the previous section, another motivation for studying island precipitation in the Maritime Continent could also be the potential relationships between past climatic changes and tectonic motions over the last several million years. Studies from Fedrov et al. (2006) show that the early climate of the Pliocene could have resembled a permanent El Niño state where sea surface temperature in the Central and Eastern Pacific were higher and the global mean air surface temperature was higher with much less surface ice (Cronin et al. 2015). A study by Dayem et al. (2007) explored the correlation between the Walker Circulation strength and compared it with precipitation from the Pacific warm pool and the Maritime Continent. Dayem et al (2007) suggested that a reorganization of the Maritime Continent in the early Pliocene could have provided the perfect conditions for the beginning of the Walker Circulation. This could have contributed to the shift to the permanent El Niño climate of the early Pliocene (Dayem et al. 2007). Furthermore, the extent of these geographical and topographical changes of the islands in the Maritime Continent and what they could have contributed to the large-scale atmospheric circulation processes over the last few million years remains an unanswered question (Cronin et al. 2015). Models like these can help us predict what might come in the future of anthropogenic climate change.

2.0 METHODS

2.1 Cloud Resolving Models

Meteorological phenomena and atmospheric circulations we observe every day can be broken down to microscale and mesoscale phenomena (Guichard and Couvreux 2017). The space and time scales of the phenomena can range from minutes to hours over meters or kilometers (Guichard and Couvreux 2017). The formation and growth of liquid water and ice particles and evaporation of raindrops make up the thermodynamic processes that form these circulations. Cloud circulations can be characterized by very strong vertical motions within the cloud that are connected with latent heat release while the clear skies around it have weaker and wider fluctuations. Modelling these highly irregular, nonlinear, phenomena can be hard. The guidance for these models is obtained from observations but observing alone isn't enough to provide explicit answers to questions about short term convective clouds.

There are 2 types of simulations used widely in the atmospheric and climate research community: a cloud resolving model, CRM, and a large eddy simulation, LES (Guichard and Couvrex 2017). In design, a LES or CRM is a numerical model that has enough grid spacing to allow the simulation to develop individual clouds whether it is over a part or the whole life cycle of the cloud. There are differences between the two in the sub-grid processes, like turbulent motions and radiative processes, but the necessary equations of motion of LES and CRMs are very similar. The distinction between the two comes essentially from the implementation of finer or coarser grids in the numerical simulations. A few hours of the simulation performing over a 10-km wide, 5-km high

domain will model a few coexisting cumulus clouds and the model is able to sample their life cycles. A longer run on the other hand, a 100-km wide, 20-km high domain and several hours of simulation become crucial when looking at deeper convective cloud cells that reach the top of the troposphere (Guichard and Couvrex 2017).

2.2 Initial Conditions

Our simulations were conducted using Cloud Model 1 (CM1) v. 19.8, which is a numerical model for studies of atmospheric processes (Bryan 2017). A large-eddy simulation (LES) closure is used for our runs. The domain of the model for our first section of runs is 512 grid points long, 256 km, and 3 grid points wide, with an island that is 62 grid points long centered in the middle of the domain from 225 to 287 grid points, seen in Figure 1. Furthermore, the grid height of our simulation is 62 vertical levels, or 31 km, which can be found in Appendix 1 under Table 1. The vertical resolution is not evenly spaced and is stretched towards the surface so the grid spacing where stretching begins was set to 100 m and the grid spacing where stretching ends was set to 500 m.

To begin, a flat control island was made with a SST of 300K with a deeper ocean temperature of 297K and a land surface temperature of 300K. The flat island simulations were run for 1,728,000 seconds, or for 20 days. During this long period of time, the model reaches an equilibrium state which is known as radiative-convective equilibrium (RCE). 3D output files were saved every hour and restart files were saved every 864,000 seconds, or every 10 days, so we had 2 restart files.

Periodic boundary conditions were imposed in both horizontal directions and no-slip boundary conditions were set at the top and bottom of the domain, meaning the wind

that passed over the island had natural friction. The simulation only had natural turbulence, no additional wind. A boundary was set on top of the system to dampen vertical cloud motion at 18000 grid boxes and the simulation was set so that the atmosphere cooled down to space and the effect of radiation was computed every 300 seconds. The latitude and longitude of the island was set to roughly simulate Sumatra at 0 degrees N and 100 degrees E. Initial surface conditions for the model represented summer.

2.3 Flat Island in a Long Channel with No Diurnal Cycle Simulations

Simulations under these conditions were run with sea surface temperatures, *tsk*, from 300K to 303K with 0.5K increments. Restart simulations were run for each of the temperatures 5 days after the initial run, day 25, in order to reduce the data and look at 2 individual days from the simulation. In addition to the 300 to 303K runs, a 20-day restart simulation was run in order to see how the diurnal cycle might continue on day 40. These flat island simulations are important because there is no diurnal cycle. This allows us to visualize what is going on above and around the island without other effects interfering with the interpretation of the results.

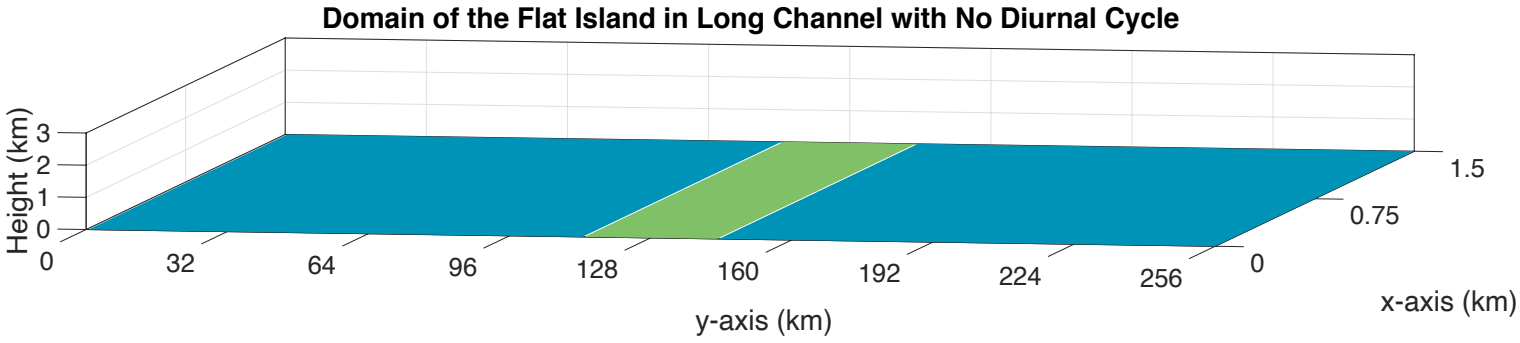

Figure 1: Domain of the flat island with no diurnal cycle. Domain of 256x1.5 km with an island that is 31x1.5 km centered in the middle of the domain. Note that the axis are not to scale.

2.4 Statistical Analysis of Flat Island with No Diurnal Cycle

In MATLAB, we performed a variety of statistical analyses to better understand what was happening to the diurnal cycle when SST rose in the restart runs. The governing equations for the model can be found in Appendix 2 in Table 2.

For potential temperature, I used the equation: $\theta = T(\frac{P0}{p})^{R/cp}$ where R is the gas constant of air and *cp* is the specific heat capacity at constant pressure. Therefore, R/cp= 0.286. *P0* is standard pressure, which is typically 1000 mb, or 100000 Pa. Pressure, *p*, and temperature, *T*, of the parcel are computed by the model. Therefore, the equation used in the script for potential temperature is: $\theta = T(\frac{100000}{p})^{0.286}$. The 5 days of the model were averaged into 1 day and plotted as a function of height and time.

In order to determine the relative humidity of an average day on the island, the saturation specific humidity needed to be calculated. The saturation specific humidity was calculated previously from a MATLAB script by Emanuel (1995). *qv* from the model is the water vapor mixing ratio which can be estimated as the specific humidity and we know that *eps*=0.622. With this in mind, we can find the relative humidity with the equation: $RH = \frac{qv}{qsat}(\frac{1 + qsat / 0.622}{1 + q / 0.622})$. An average of the 5 days of the model was computed and plotted as a function of height and time.

Cloudiness was computed by adding *qc*, the mixing ratio of cloud liquid water, and *qi*, the mixing ratio of cloud ice. The 5 days of the model are averaged to one day and it is plotted as a function of height and time. The mixing ratio of water vapor, *qv*, was averaged over the 5 days of the model and plotted as a function of height and time.

Horizontal velocity, u, meridional velocity, v, and vertical velocity, w, are averaged over the 5 days of the model and plotted as a function of height and time.

Rainfall accumulation is computed directly from the model. Rainfall rate can be calculated by taking the average of the rainfall accumulation over time and plotting it as a function of time.

2.5 Flat Island with Diurnal Cycle Simulations

Following these short runs and statistical analysis, a high *u* value was found at 5 km altitude in the 300K run. This feature is possibly a result of the interaction between convection and gravity waves and, while interesting in its own sake, it creates conditions that are not typical in the Maritime Continent. Thus, in order to mitigate this horizontal jet, the dimensions of the domain and the island size were changed. Due to the dimensions of our previous island, it was hypothesized that the jet appeared from the long channel, so the domain was changed from 512x3 grid points to 128x128 grid points, or 64x64 km. The SST was left at 300K and the model was run for 518,400 seconds, or for 6 days. Following the changing domain, the island size was changed from 62x3 grid points to 32x128 grid points to get an island that is 16x64 km, seen in Figure 2. This produced a long run that we were able to use as the control and the same conditions for 300K to 303K with 0.5K increments were run. For this simulation, the diurnal cycle of radiation was included, and the horizontal jet did not appear. The same statistical analysis tests were run on this new island as the previous flat island.

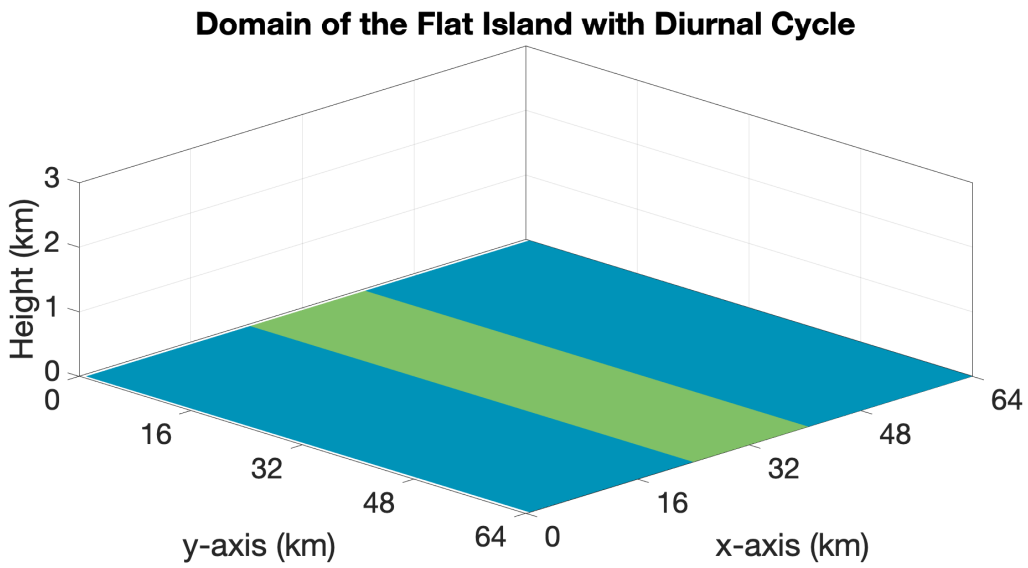

Figure 2: Domain of the flat island with a diurnal cycle. Domain of 64x64 km with an island that is 16x64 km centered in the middle of the domain.

2.6 Statistical Analysis of Flat Island with Diurnal Cycle

In MATLAB, the same statistical analysis tests were performed as on the flat island with no diurnal cycle. The averages for potential temperature, mixing ratio of water vapor, relative humidity, rainfall rate, cloud water and cloud ice, vertical, zonal, and meridional velocity were calculated. Furthermore, we calculated the surface temperature of the island to better visualize how the solar radiation impacted the heating of the land. The results for these variables for all of the SSTs between 300 K and 303 K were calculated and plotted to compare.

2.7 Mountainous Island with Diurnal Cycle Simulations

The same conditions were run on the mountainous island, but a bell-shaped hill was added. The simple mountain is 1 km tall and 2 km wide, similar to the size of the mountain range in Sumatra. This bell-shaped hill extends the length of the domain. Therefore, the ocean will have a slight slope since it is part of the edge of the bell curve.

This is a numerical artifact due to the construction of the domain, but the slope outside of the island is small enough that it does not have significant effects on the atmospheric circulation. The same conditions from the new flat island were used for the mountainous island so the domain was 128x128 grid boxes, or 64x64 km, with an island that is 32x128 grid points, or 16x64 km, centered in the model seen in Figure 3. Using this setup, simulations were run from 300K to 303K with increments of 0.5K. 3D output files were saved every 12 hours and restart simulations were run 5 days after the simulation finished, day 25 of the model, to better view the equilibrium the model reached.

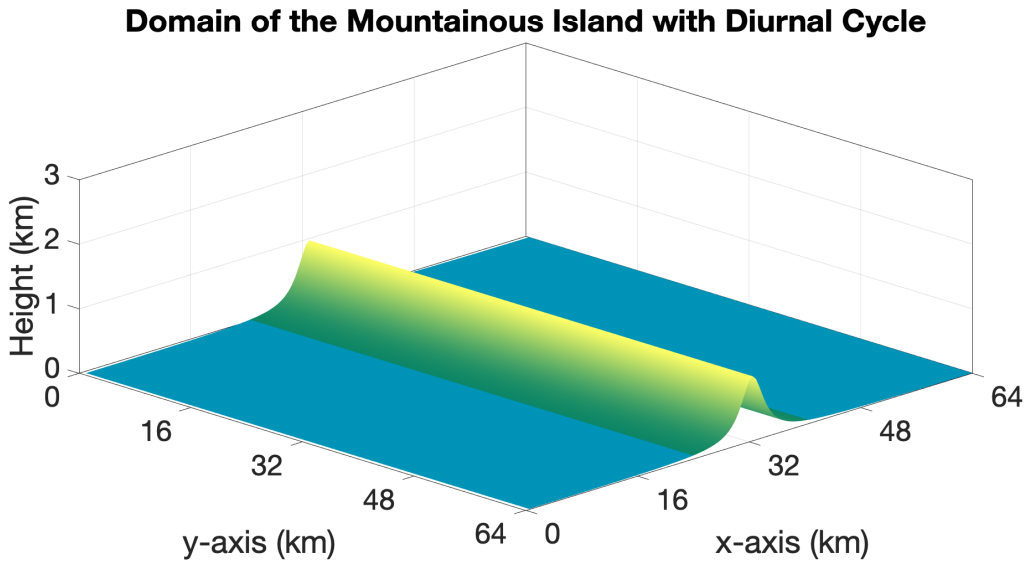

Figure 3: Domain of the mountainous island with a diurnal cycle. Domain of 64x64 km with an island that is 16x64 km centered in the middle of the domain with a mountain 1 km high.

2.8 Statistical Analysis of Mountainous Island with Diurnal Cycle

Using the restart files from the mountainous island at 300K to 303K, the same statistical analysis was run on these output files as the flat islands. Water vapor mixing ratio, horizontal velocity, meridional velocity, vertical velocity, potential temperature, relative humidity, cloudiness, surface temperature, and rainfall rate were averaged over the 5 days of the simulation and plotted as a function of height and time.

Using this data, we can compare it to the flat island to see how changing the SST and the topography of the island affects the cloud formations, precipitation, and diurnal cycle of convection of the islands.

3.0 RESULTS

3.1 Flat Island in Long Channel with No Diurnal Cycle Control

3 points were chosen from the domain: one from the middle of the island at 128 km, one near the coast of the island at 112.5 km, and one farther into the ocean at 90 km to see what patterns took place above and around the long island with no diurnal cycle, seen in Figure 1.

3.1.1 Middle of the Island

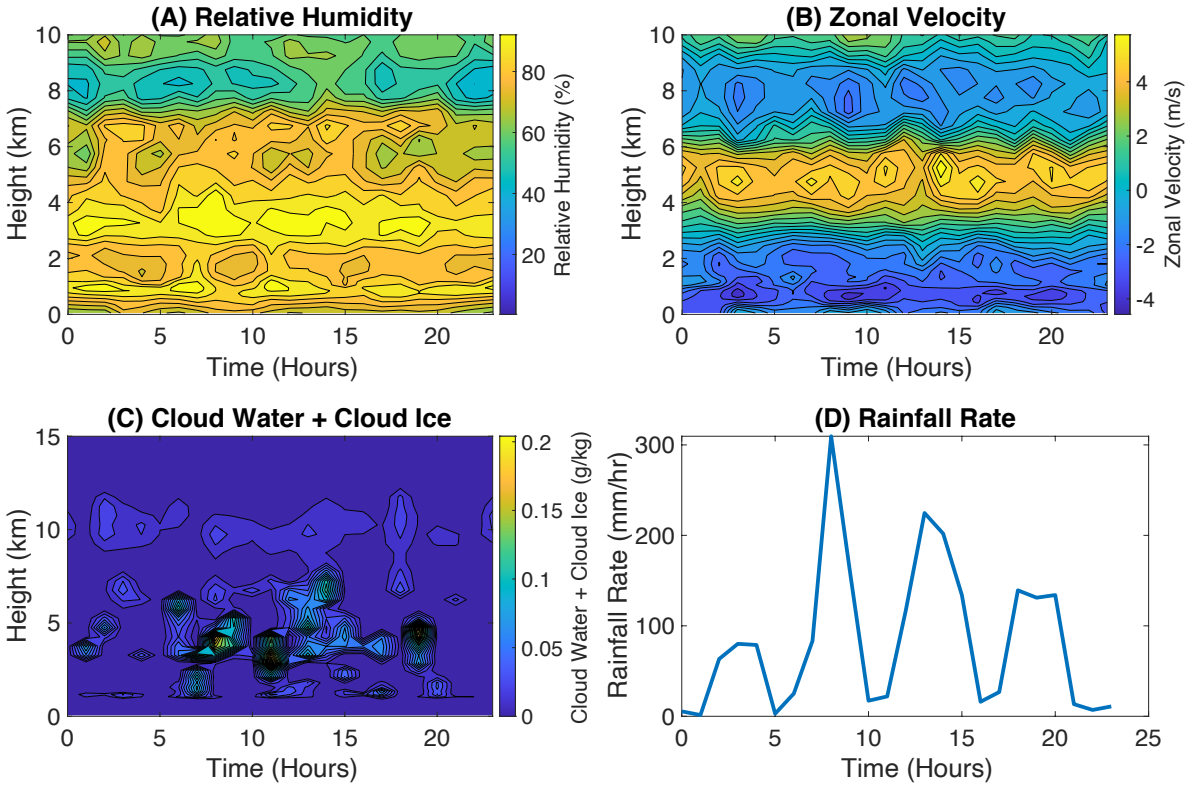

Figure 4: (A) Relative humidity throughout the average 300K day in the middle of the flat island with no diurnal cycle in %. (B) The zonal velocity throughout the average 300K day in the middle of the flat island with no diurnal cycle in m/s.. (C) Cloud coverage throughout the average 300K day in the middle the flat island with no diurnal cycle in g/kg. (D) Rainfall rate throughout the average 300K day in the middle of the flat island with no diurnal cycle in mm/hr.

At 128 km in the middle of the island, rainfall rate peaks at 9:00 with 300 mm/hr and at 14:00 with a rate of 220 mm/hr, seen in Figure 4 (D). There are 2 smaller peaks at 4:00 and 20:00. The mixing ratio of water vapor, *qv*, at the surface, peaks at 14 g/kg at 5:00, 10:00, and 20:00 with a gradual decrease in mixing ratio with height (not shown). There is a strong zonal velocity of 4-5 m/s at 5 km in Figure 4 (B). The cause of this jet is beyond the scope of this work, but we hypothesized it is likely a result of the interaction between convection and large-scale phenomena, such as gravity waves, that develop in the model during the simulation. There is not much large-scale vertical or meridional velocity throughout the average day with a SST of 300K (not shown). The relative humidity peaks at around 95% between 2:00-3:00 at 1 and 3 km as seen in Figure 4 (A). Then, it peaks again from 7:00 to 8:00 at 1 and 3 km. There is a smaller window of 95% relative humidity at 12:00 at 1 km, but the relative humidity at 3 km at this same time lasts for longer. Lastly, there is another peak of 95% relative humidity between 18:00 and 20:00 at 1 and 3 km. Clouds form at 1 and 3 km at 3:00 and 4:00 shown in Figure 4 (C). Much deeper clouds start to form at 8:00 at 1 and 3 km. At 12:00, the 1 km and 3 km clouds seem to touch and form a large, deep cloud. At 18:00 there are smaller clouds mixing ratios at 1 km and 3 km and then at 20:00 there are small values of cloud mixing ratios that extend upward by a few kilometers.

3.1.2 Island Coast

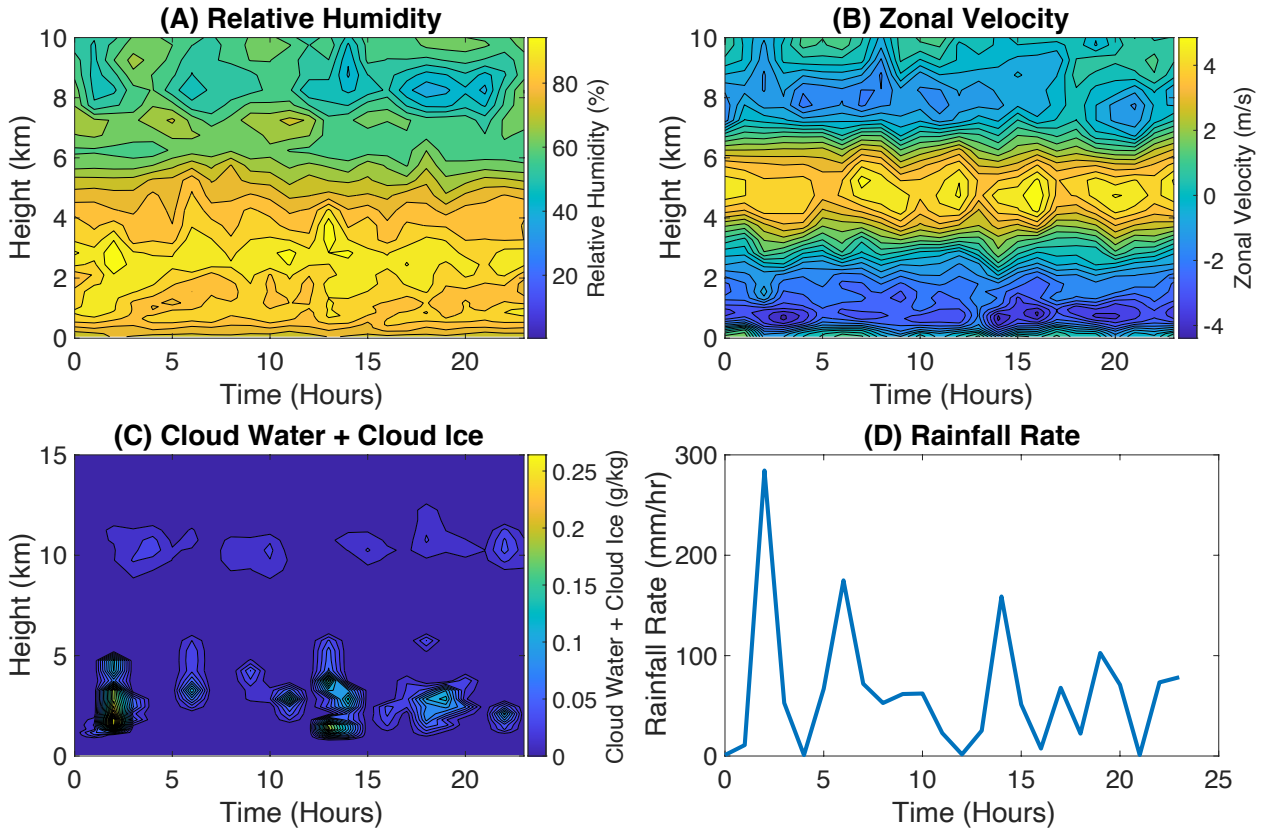

Figure 5: (A) Relative humidity throughout the average 300K day on the coast of the flat island with no diurnal cycle in %. (B) The zonal velocity throughout the average 300K day on the coast of the flat island with no diurnal cycle in m/s. (C) Cloud coverage throughout the average 300K day on coast of the flat island with no diurnal cycle in g/kg. (D) Rainfall rate throughout the average 300K day on the coast of the flat island with no diurnal cycle in mm/hr.

At 112.5 km on the coast of the island, rainfall rate is the highest at 3:00 with 280 mm/hr of rainfall, shown in Figure 5 (D). There are two smaller peaks of rainfall at 7:00 and 15:00 with approximately 160 mm/hr of rainfall and then two small showers follow late in the evening at 18:00 and 20:00 around 100 mm/hr of rain. The mixing ratio of water vapor remains relatively steady throughout the day, decreasing with altitude (not shown). The mixing ratio is 13.7 g/kg close to the surface throughout the day but has a few peaks that correlate with the rainfall rate. There is a horizontal jet around 5 km similar to the middle of the island at 225 km in Figure 5 (B). There is not much

meridional velocity throughout the average day on the coast of the island, but there is a little more vertical velocity than in the middle of the island. There is 0.5 m/s of vertical velocity at 3:00 in correspondence to the highest amount of rain (not shown). This is likely the manifestation of the updraft that gave rise to a cloud at that time. Clouds seem to develop in many parts of the day, which is indicated by the amount of rainfall as well, shown in Figure 5 (C).

3.1.3 Ocean

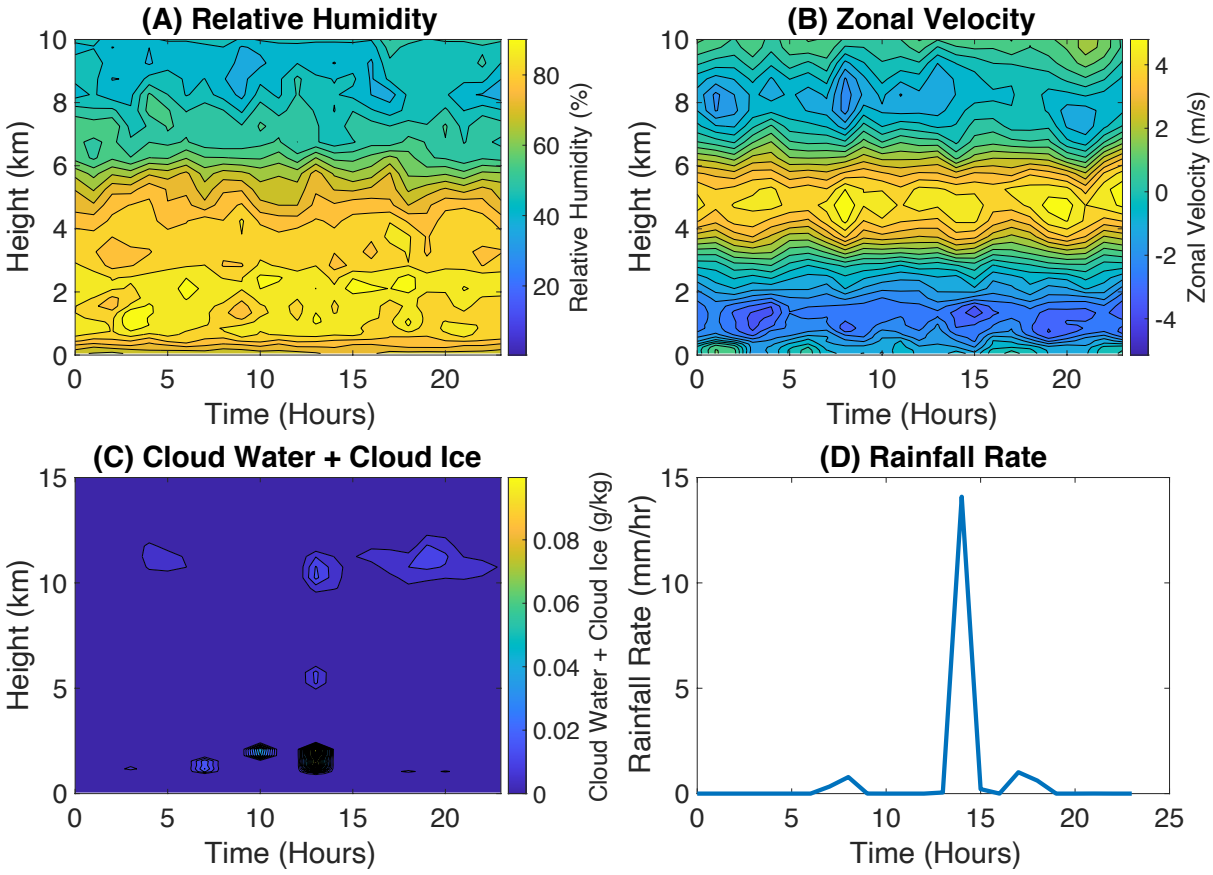

Figure 6: (A) Relative humidity throughout the average 300K day over the ocean of the flat island with no diurnal cycle in %. (B) The zonal velocity throughout the average 300K day over the ocean of the flat island with no diurnal cycle in m/s. (C) Cloud coverage throughout the average 300K day over the ocean of the flat island with no diurnal cycle in g/kg. (D) Rainfall rate throughout the average 300K day over the ocean of the flat island with no diurnal cycle in mm/hr.

At 90 km in the middle of the ocean, rainfall rate is relatively low compared to rainfall rate on and closer to the island, shown in Figure 6 (D). At 15:00 rainfall rate is 15 mm/hr and there is negligible rainfall the rest of the day. The mixing ratio of water vapor is around 13.4 g/kg on the surface and stays relatively constant, then decreases with altitude (not shown). Similar to the middle of the island, there is a horizontal jet 5 km high shown in Figure 6 (B), and negligible meridional and large-scale vertical velocity (not shown). Relative humidity stays relatively constant throughout the day, shown in Figure 6 (A). Starting at 72% at the surface, relative humidity reaches 90-95% around 1 km at the cloud base, or LCL, and then slowly decreases to 41% at 10 km. The rest of the average day is similar. At 14:00 clouds form between 1 and 2.5 km but the rest of the day is mostly clear which is shown in Figure 6 (C). Potential temperature is similar to the middle of the island and the coast where it is 297 K at the surface, and it slowly increases with height to 314 K at 5 km, shown in Figure 9 (B).

3.2 Climate Change Runs of Flat Island in Long Channel with No Diurnal Cycle

The SST was increased from 300K to 303K in 0.5K intervals. The average day of all 7 SSTs in the middle of the islands, on the coast of the islands, and over the oceans, were plotted for each of the variables in order to compare the results.

3.2.1 Middle of the Island

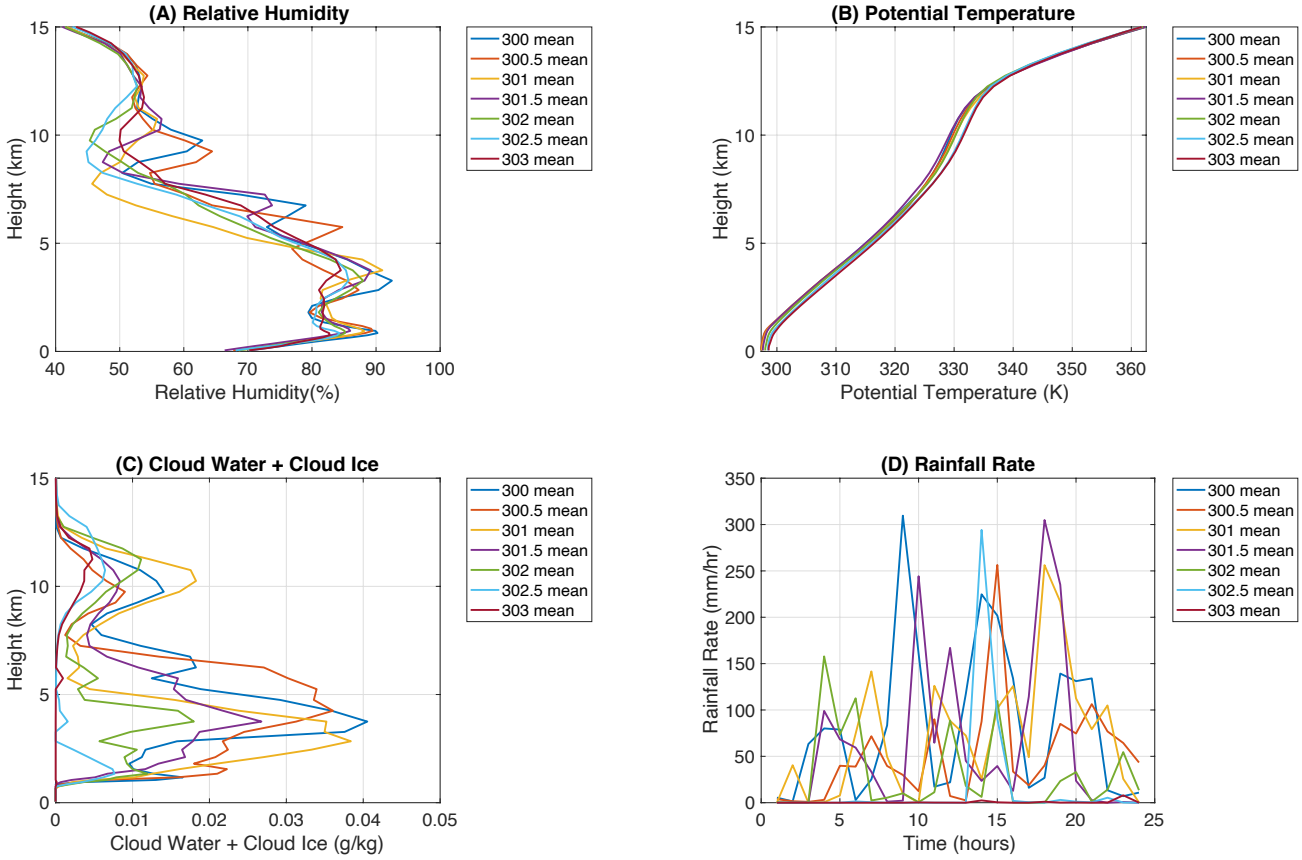

Figure 7: (A) The mean relative humidity for SSTs of 300K, 300.5K, 301K, 302.5K, 302K, and 303K on the average day in the middle of the flat island with no diurnal cycle in %. (B) The mean potential temperature for SSTs of 300K, 300.5K, 301K, 302.5K, 302K, and 303K on the average day in the middle of the flat island with no diurnal cycle in K. (C) Mean cloud coverage for SSTs of 300K, 300.5K, 301K, 302.5K, 302K, and 303K on the average day in the middle of the flat island with no diurnal cycle in g/kg. (D) The mean rainfall rate for SSTs of 300K, 300.5K, 301K, 302.5K, 302K, and 303K on the average day in the middle of the flat island with no diurnal cycle in mm/hr.

As temperature increased, the mixing ratio of water vapor, *qv*, has a similar pattern between the 7 SSTs, but there is a difference of 3 g/kg of near the surface (not shown). This difference lessens as height increases. There are large variations in relative humidity, especially between 2 and 12 km and it seems to follow a pattern as SST increases which can be seen in Figure 7 (A). Horizontal velocity is variable between the 7 SSTs, each with different peaks of horizontal velocity at varying heights.

As mentioned above, a large jet appears at 5 km in all of the average days, but it is most prominent in the 303 K run, and another jet appears in the average 300.5 K day at 11 km. Average vertical velocity and meridional velocity are variable between the SSTs as well, but it is clear that there is strong upwelling in the 300.5 K average day at 6.3 km.

The potential temperature takes on the same pattern for each of the SSTs on the coast of the island which can be seen in Figure 7 (B). In all of the SSTs, rainfall takes place around the same time of day, but the duration and the rainfall rate vary between different runs, shown in Figure 7 (D). 300 K has the highest rainfall rate of 320 mm/hr at 9:00, but 302.5 K reaches 290 mm/hr at 14:00 and 301.5 K reaches 310 mm/hr at 17:00. Cloud formations are similar between the 7 SSTs with low clouds at 4 to 6 km and clouds higher up in the atmosphere between 8 and 12 km, shown in Figure 7 (C). In general, as SST rises, there are less clouds over the island.

3.2.2 Island Coast

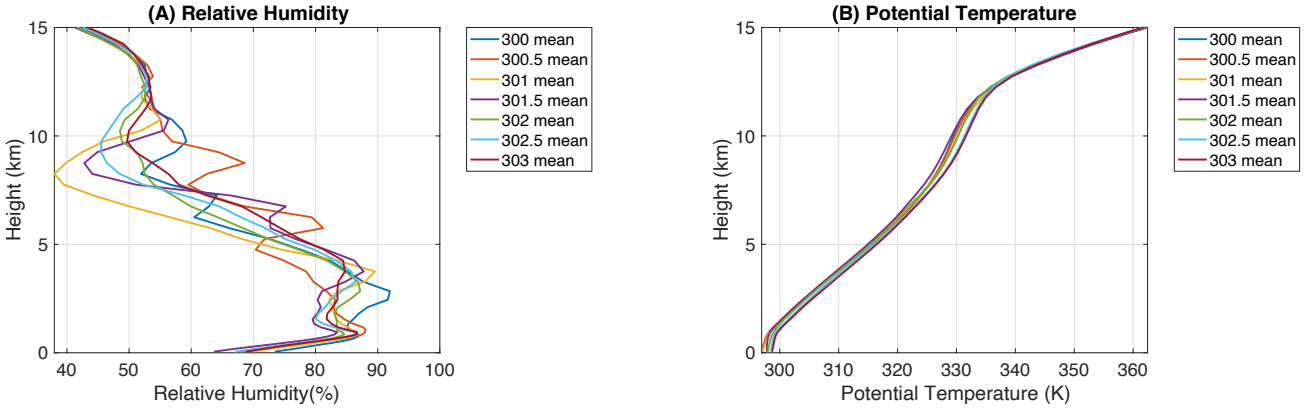

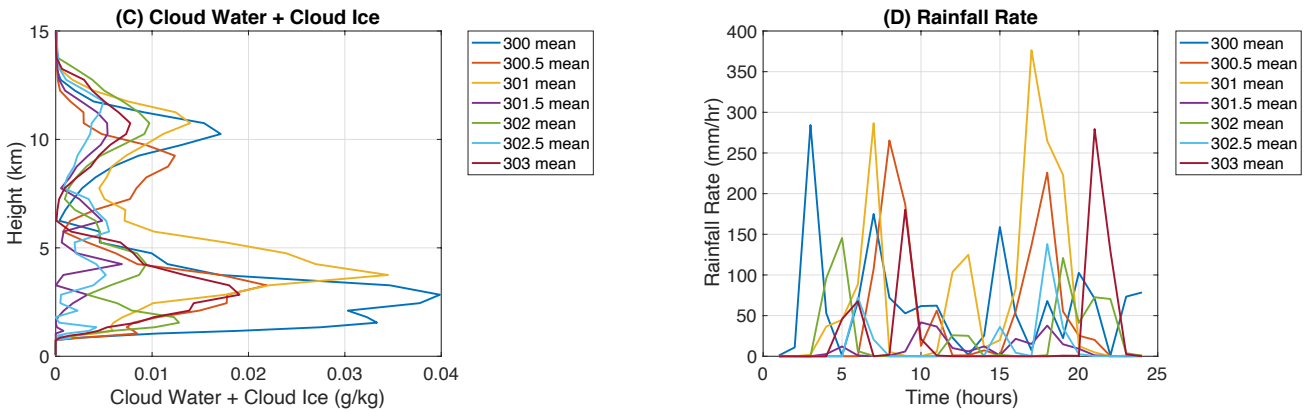

Figure 8: (A) The mean relative humidity for SSTs of 300K, 300.5K, 301K, 302.5K, 302K, and 303K on the average day on the coast of the flat island with no diurnal cycle in %. (B) The mean potential temperature for SSTs of 300K, 300.5K, 301K, 302.5K, 302K, and 303K on the average day on the coast of the flat island with no diurnal cycle in K. (C) Mean cloud coverage for SSTs of 300K, 300.5K, 301K, 302.5K, 302K, and 303K on the average day on the coast of the flat island with no diurnal cycle in g/kg. (D) The mean rainfall rate for SSTs of 300K, 300.5K, 301K, 302.5K, 302K, and 303K on the average day on the coast of the flat island with no diurnal cycle in mm/hr.

On the coast of the island, the mixing ratio of water vapor takes on the same pattern between all of the SSTs, varying by about 3 g/kg at the surface. The relative humidity is variable between the SSTs, shown in Figure 8 (A). All of the islands reach a maximum relative humidity between 85% to 92% 2 to 4 km high in the atmosphere and then relative humidity begins to decrease after that, but at varying rates. 301 K reaches the lowest relative humidity of 37% at 8 km. As the relative humidity decreases, there are small spikes as height increases in the runs with lower SSTs. Horizontal velocity follows almost the exact same pattern as it does in the middle of the island at 256 km where 303 K peaks at 6 km with 5.8 m/s and another peak in horizontal velocity in the 300.5 K island of 5.8 m/s at 11 km. Vertical velocity is greatest in 301 K and 300.5 K, the 301 K SST reaching 0.1 m/s at 4.8 km.

Potential temperature follows the same pattern for all of the mean SSTs, but 302.5 K and 303 K are slightly warmer than the other temperatures by a few degrees between 6

and 12 km. As the SST warms, cloud coverage decreases, shown in Figure 8 (C). There are the most low clouds in the 300 K island at 0.04 g/kg at 3 km, and as the surface temperature warms, the low cloud coverage decreases. There is a set of higher clouds consistent with all of the SSTs around 12 km, but 300 K still has the most and as the SST warms, the coverage decreases.

Rainfall rate is variable between the SSTs, all peaking at different times of the day, shown in Figure 8 (D). 301 K reaches the highest rainfall rate of 370 mm/hr at 17:00.

3.2.3 Ocean

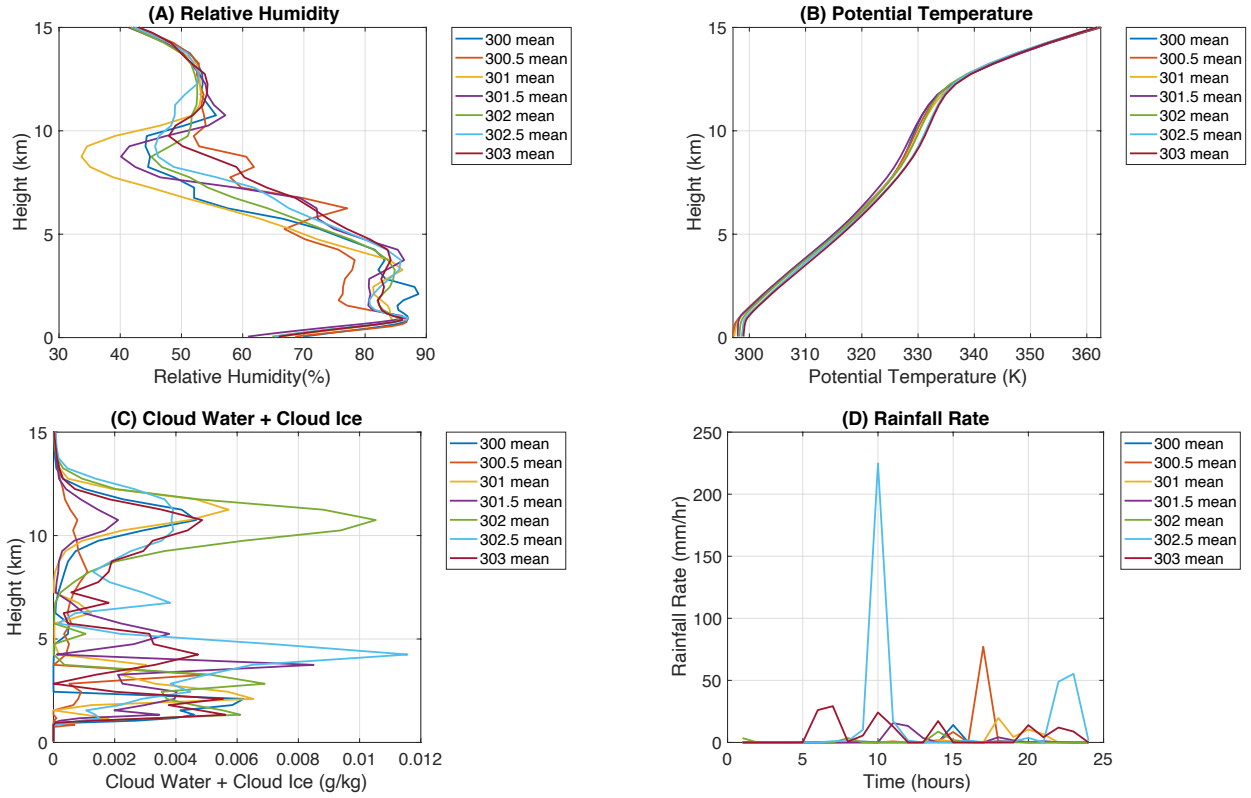

Figure 9: (A) The mean relative humidity for SSTs of 300K, 300.5K, 301K, 302.5K, 302K, and 303K on the average day over the ocean of the flat island with no diurnal cycle in %. (B) The mean potential temperature for SSTs of 300K, 300.5K, 301K, 302.5K, 302K, and 303K on the average day over the ocean of the flat island with no diurnal cycle in K. (C) Mean cloud coverage for SSTs of 300K, 300.5K, 301K, 302.5K, 302K, and 303K on the average day over the ocean of the flat island with no diurnal cycle in g/kg. (D) The mean rainfall rate for SSTs of 300K, 300.5K, 301K, 302.5K, 302K, and 303K on the average day over the ocean of the flat island with no diurnal cycle in mm/hr.

Over the ocean, the mixing ratio of water vapor varies a little more on the surface between SSTs, but they all have the same pattern that decrease with height. Relative humidity is similar to the coast of the islands, but 301 K drops to 32% at 8 km, seen in Figure 9 (A). There is a negative vertical velocity of -0.05 m/s at 3 km and then soon after at 4 km there is a vertical velocity of 0.03 m/s (not shown). This is a very small difference, and the other runs have an even smaller one. There is a vertical velocity of 0.038 m/s at 11.5 km over the 301 K SST island. Horizontal velocity is variable between the different SSTs but there is still a strong horizontal velocity of 5.8 m/s 6 km high in the 303 K ocean and a velocity of 5.3 m/s 11.5 km high in the 300.5 K ocean.

Potential temperature follows the same pattern as over the coast of the islands, with 302.5 K and 303 K slightly warmer than the rest of the ocean's temperatures shown in Figure 9 (B). Rainfall decreases greatly over the ocean and the most rainfall occurs in the 302.5 K ocean with 230 mm/hr at 10:00, with a small shower from 22:00 to 23:00, shown in Figure 9 (D). At 4 km, the 302.5 K ocean has the most cloud coverage of 0.011 g/kg which can be seen in Figure 9 (C). The other SSTs have low clouds but not very many of them. Higher in the atmosphere there are clouds at 11 km over the 302 K ocean.

3.3 Flat Island with Diurnal Cycle Control

The new, modified simulation is 64x64 km with an island that is 16x64 km seen in Figure 2, so measurements in the same places on the island were taken to compare the differences between a flat island with and without a diurnal cycle of convection.

3.3.1 Middle of the Island

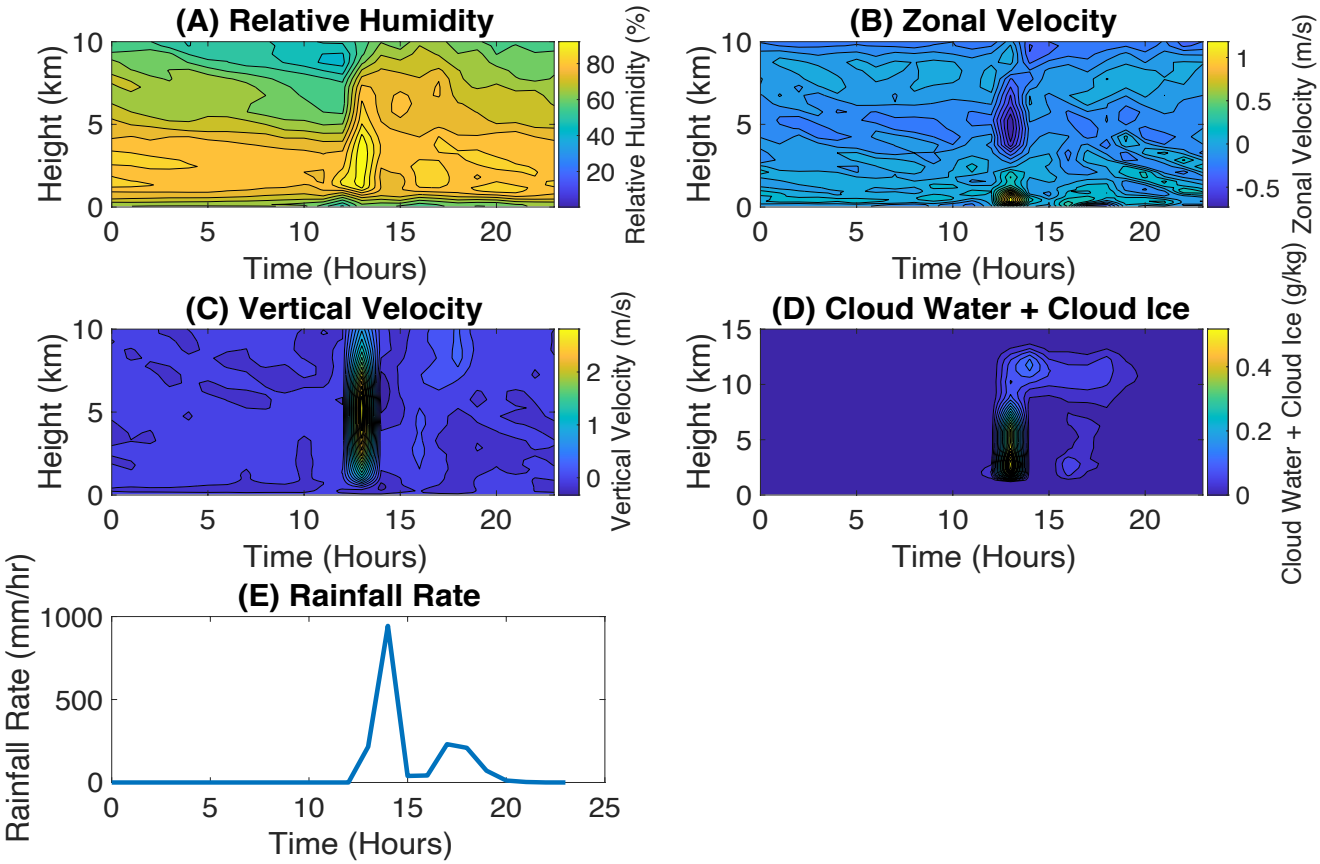

Figure 10: (A) Relative humidity throughout the average 300K day in the middle of the flat, diurnal island in %. (B) The zonal velocity throughout the average 300K day in the middle of the flat, diurnal island in m/s. (C) The vertical velocity throughout the average 300K day in the middle of the flat, diurnal island in m/s. (D) Cloud coverage throughout the average 300K day in the middle of the flat, diurnal island in g/kg. (E) Rainfall rate throughout the average 300K day in the middle of the flat, diurnal island in mm/hr.

As shown in Figure 13 (C), the control island with a diurnal cycle at 32 km, has a surface temperature that starts at 295 K, cooling throughout the early morning, then rising again at 8:00 to peak at 12:00 with 303 K. There is a slight dip in the surface temperature at 14:00 to 299 K, when the precipitation takes place. This is likely a result of the evaporative cooling that follows the fall of precipitation in an unsaturated atmosphere.

Temperature warms again at 16:00 to 302 K and cools throughout the rest of the evening and nighttime.

There is no rainfall throughout the morning on the island and at 14:00, but there is a spike in rainfall rate at 990 mm/hr that quickly stops, seen in Figure 10 (E). Then at 17:00, there is much less rainfall at a rate of 200 mm/hr, lasting an hour.

At 14:00, the potential temperature warms from 297 degrees K to 299.7 degrees K at the surface and cools again at 16:00. At 13:00, clouds start to form stretching from 1.3 km to 13.25 km, with the largest of 0.5 g/kg at 2.8 km, shown in Figure 10 (D).

At 16:00, cloud mixing ratios suggest that clouds are shallower than those that happened earlier, stretching roughly between 1.5 km to 7.25 km with a mixing ratio of 0.07 g/kg.

At 13:00, relative humidity becomes 94% at 1.3 km where the base of the cloud begins, but remains at 64% on the surface, seen in Figure 10 (A).

There is a strong positive vertical velocity of 2.2 m/s 13:00 which can be seen in Figure 10 (C). The vertical velocity begins at 550 m and stretches upward past 10 km. Meridional velocity is mostly negligible. At 13:00 the horizontal velocity increases to 1 m/s near the surface and becomes -0.7 m/s higher up in the atmosphere from 3 km to 7.75 km, shown in Figure 10 (B). The behavior of zonal velocity near the surface is likely the result of land-sea breezes and outflows from the deep convection that develops throughout the day.

3.3.2 Island Coast

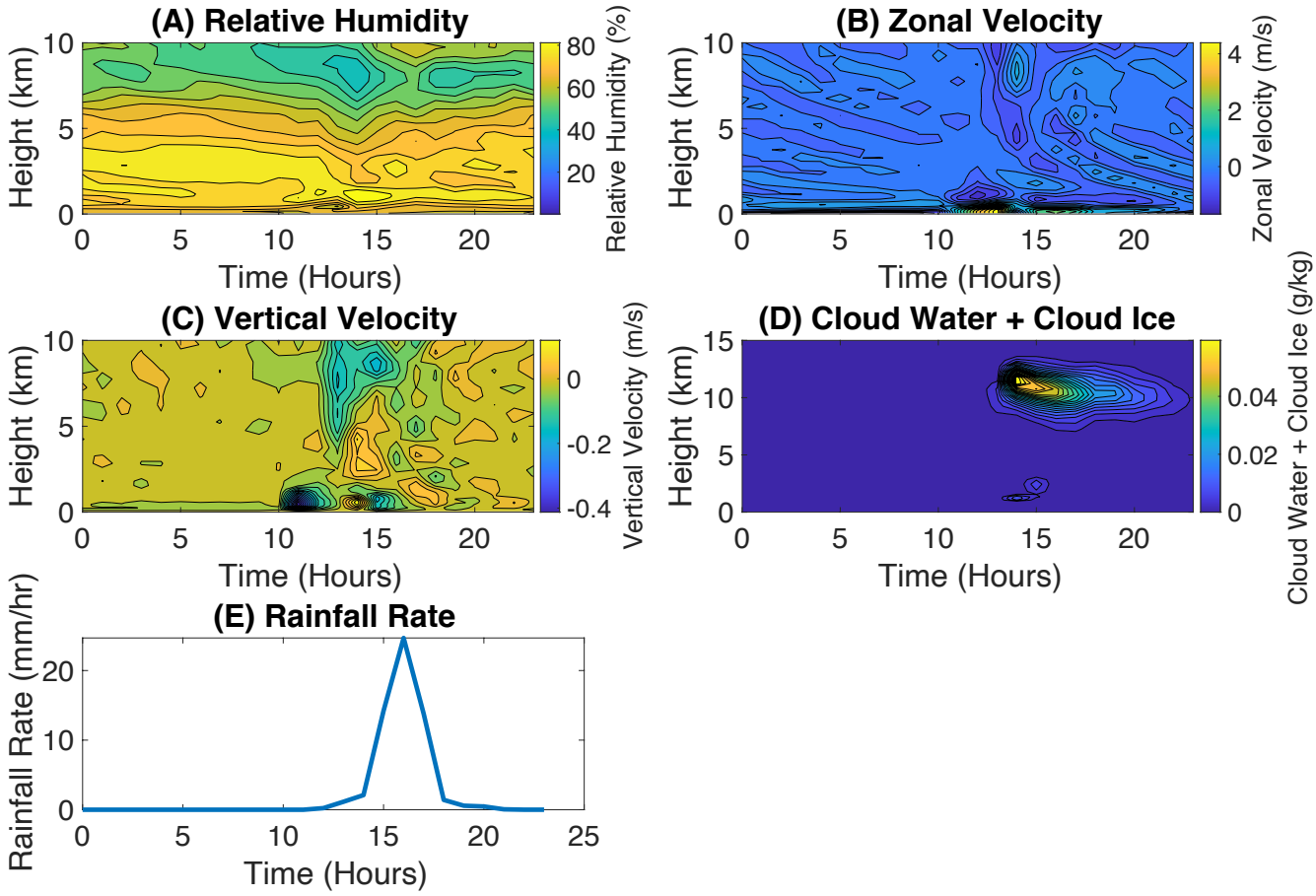

Figure 11: (A) Relative humidity throughout the average 300K day on the coast of the flat, diurnal island in %. (B) The zonal velocity throughout the average 300K day on the coast of the flat, diurnal island in m/s. (C) The vertical velocity throughout the average 300K day on the coast of the flat, diurnal island in m/s. (D) Cloud coverage throughout the average 300K day on the coast of the flat, diurnal island in g/kg. (E) Rainfall Rate throughout the average 300K day on the coast of the flat, diurnal island in mm/hr.

On the coast of the island, the surface temperature reaches its lowest point at 8:00 just below 297 K which can be seen below in Figure 14 (C). Then it rises throughout the morning to approximately 301 K between 11:00 and 15:00, with a slight drop at 14:00. After 15:00, the temperature lowers throughout the evening and nighttime until it reaches its lowest point at 8:00 the next day. The maximum relative humidity is reached from 14:00 to 15:00 of 80% at 1 km, seen in Figure 11 (A).

On the surface throughout the average day, the relative humidity stays around 65% and decreases with height. There is very low horizontal velocity throughout the day but at 13:00, there is strong horizontal movement of 4.3 m/s at the surface which quickly dies off, seen in Figure 11 (B). Vertical velocity remains low throughout the day as well but at 11:00 at the surface, the is a strong negative vertical velocity, followed by positive vertical velocity at 14:00 which can be seen in Figure 11 (C). At 14:00, there is a large cloud high up in the atmosphere between 8 and 13 km that is spreading from the interior of the island, lasting until 24:00, shown in Figure 11 (D).

There is a small, low hanging cloud that forms at 14:00 and 15:00. At 16:00. There is 25 mm/hr of rainfall and that is the only shower throughout the average day on the coast of the 300 K island which can be seen in Figure 11 (E).

3.3.3 Ocean

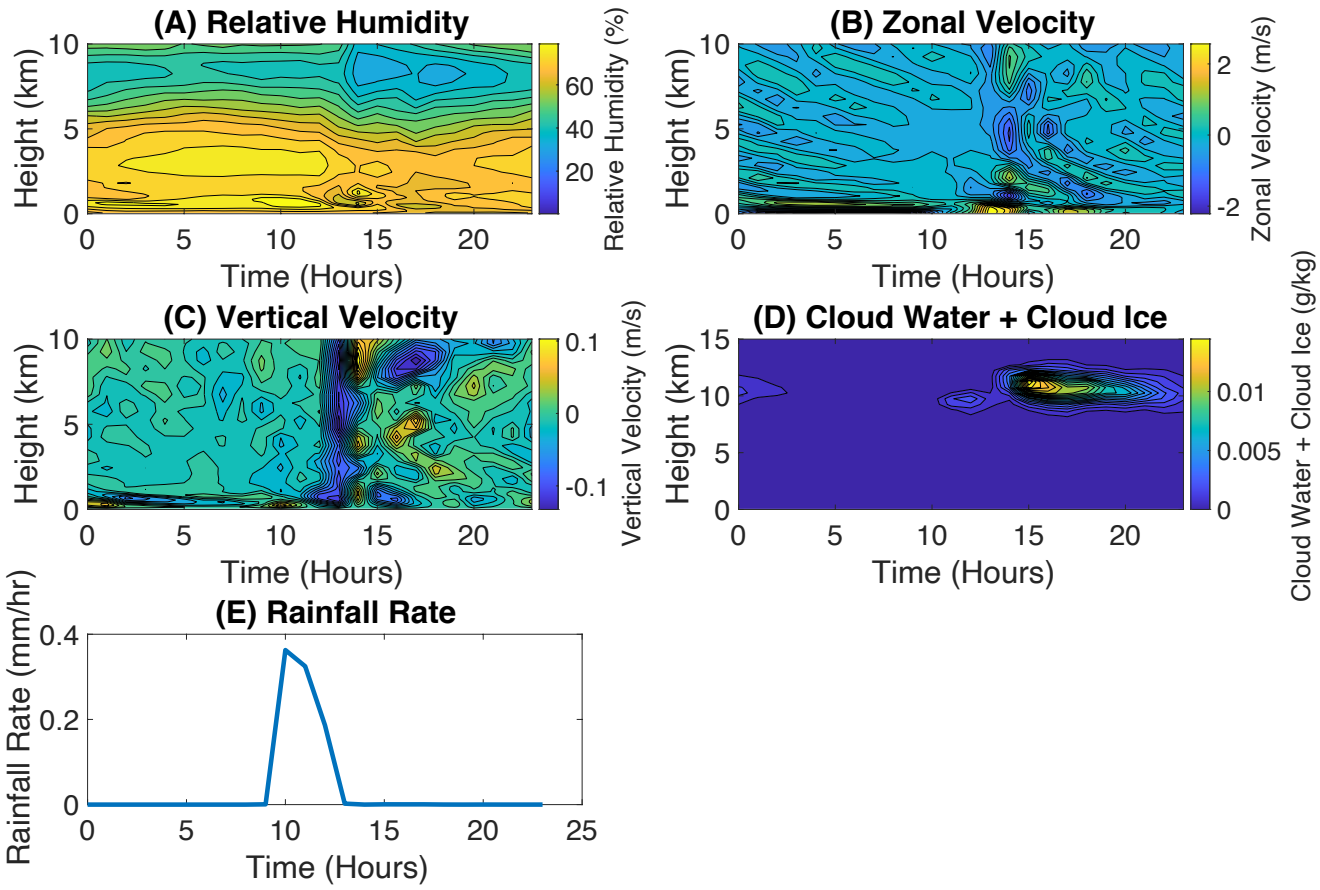

Figure 12: (A) Relative humidity throughout the average 300K day over the ocean of the flat, diurnal island in %. (B) The zonal velocity throughout the average 300K day over the ocean of the flat, diurnal island in m/s. (C) The vertical velocity throughout the average 300K day over the ocean of the flat, diurnal island in m/s. (D) Cloud coverage throughout the average 300K day over the ocean of the flat, diurnal island in g/kg. (E) Rainfall rate throughout the average 300K day over the ocean of the flat, diurnal island in mm/hr.

Over the ocean, surface temperature remains constant at 300 K because there is no surface heating throughout the day over the ocean (not shown). There is low horizontal velocity throughout the day, but at 13:00, there is a small gust wind at the surface of the ocean of 2.3 m/s and a smaller gust at 17:00, seen in Figure 12 (B). The former is likely a result of the convergence that is developing over the heated island, while the latter is probably due to convective outflows that develop on the island and the coast in the later parts of the afternoon.

Vertical velocity remains relatively constant throughout the day with two small vertical gusts at the surface of the ocean at 1:00 and 10:00, shown in Figure 12 (C). At 13:00 there is a strong negative vertical velocity from the surface of the ocean, stretching to the top of the troposphere.

Clouds form high up in the atmosphere between 9 and 13 km starting at 10:00, but the most clouds form at 15:00 which can be seen in Figure 12 (D). These clouds stay high up in the atmosphere throughout the night and are gone by 3:00. There is minimal rainfall, with a small peak of 0.4 mm/hr at 10:00 that is shown in Figure 12 (E).

3.4 Climate Change Runs of the Flat Island with Diurnal Cycle

The SST was increased from 300K to 303K in 0.5 K intervals and the averages of these were plotted as a function of height and time in order to compare results between a flat island with and without a diurnal cycle.

3.4.1 Middle of the Island

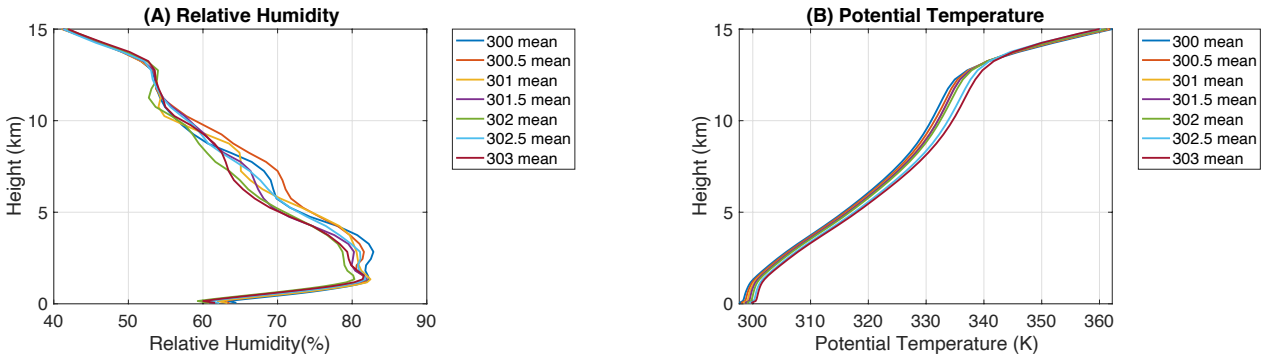

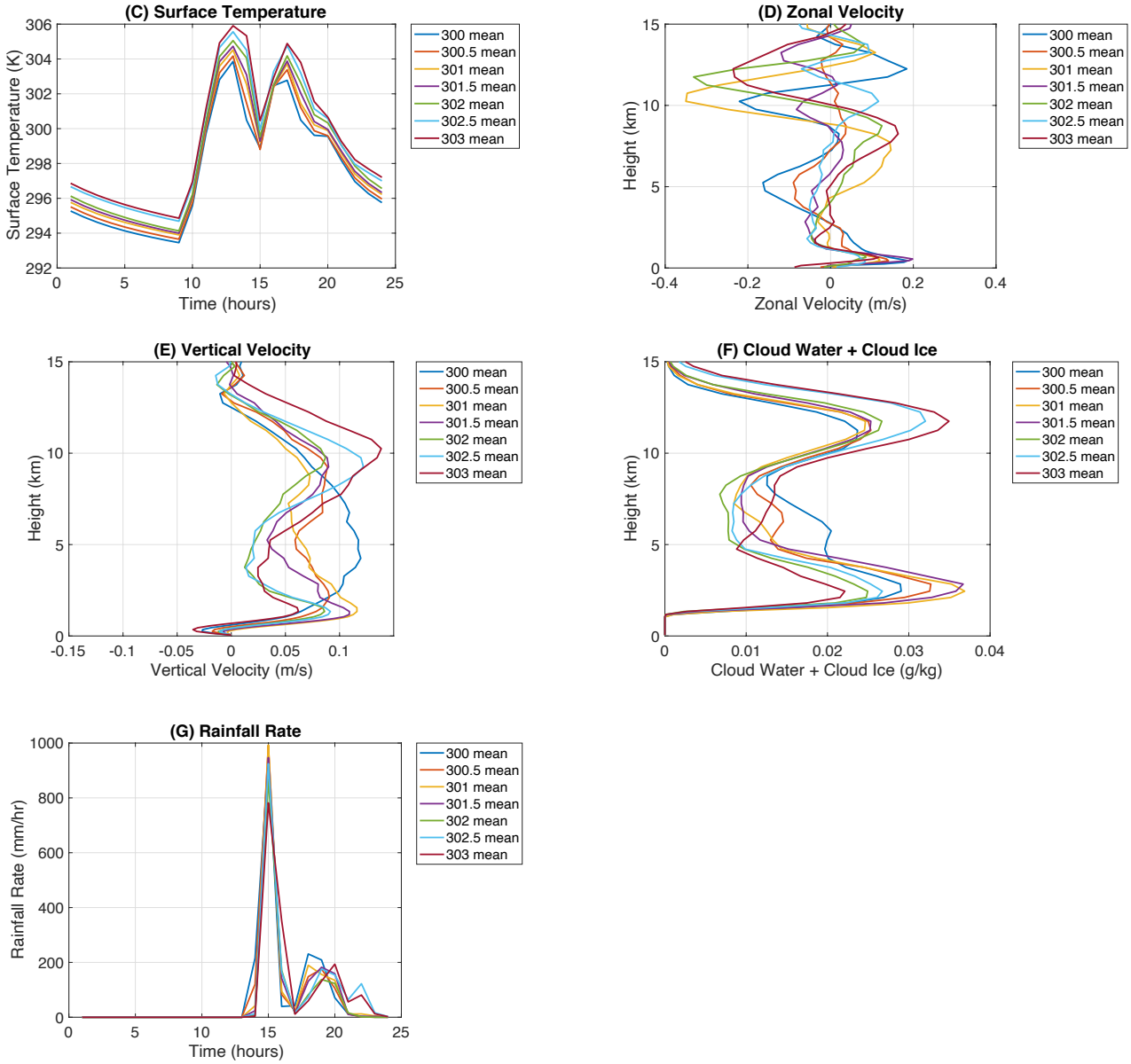

Figure 13: (A) The mean relative humidity for SSTs of 300K, 300.5K, 301K, 302.5K, 302K, and 303K on the average day in the middle of the flat, diurnal island in %. (B) The potential temperature for SSTs of 300K, 300.5K, 301K, 302.5K, 302K, and 303K on the average day in the middle of the flat, diurnal island in K. (C)The mean land surface temperature for SSTs of 300K, 300.5K, 301K, 302.5K, 302K, and 303K on the average day in the middle of the flat, diurnal island in K. (D) The mean zonal velocity for SSTs of 300K, 300.5K, 301K, 302.5K, 302K, and 303K on the average day in the middle of the flat, diurnal island in m/s. (E) The mean vertical velocity for SSTs of 300K, 300.5K, 301K, 302.5K, 302K, and 303K on the average day in the middle of the flat, diurnal island in m/s. (F) Mean cloud coverage for SSTs of 300K, 300.5K, 301K, 302.5K, 302K, and 303K on the average day in the middle of the flat, diurnal island in g/kg. (G) The mean rainfall rate for SSTs of 300K, 300.5K, 301K, 302.5K, 302K, and 303K on the average day in the middle of the flat, diurnal island in mm/hr.

The diurnal cycle in the middle of the flat, smaller island at 32 km has a surface temperature that reaches its coolest point at 9:00 of between 293.5 K and 294.9 K, seen in Figure 13 (C). Then throughout the late morning the temperature rises, reaching the highest temperature at 13:00 of between 303.9 K and 305.9 K. Following, at 15:00, there is a dip in temperature ranging between 298.8 K and 300.5 K with another smaller rise in temperature at 17:00 between 302.8 K and 304.9 K. After this, the temperature slowly decreases throughout the evening and nighttime, becoming the coolest at 9:00 again the next day and this is consistent with all of the SST runs between 300 K and 303 K. The drop in temperature at 15:00 correlates with the spike in rainfall rate of between 700 mm/hr and 990 mm/hr which can be seen in Figure 13 (G). Furthermore, as SST increases, there is a delay in the first and secondary maxima of rainfall. This is consistent with the hypothesis that the drop is due to evaporative cooling of rainfall. Following the peak in rainfall, each of the SST runs have a secondary maximum that follows between 18:00 and 22:00. With warmer SSTs, the secondary maxima are slightly higher, and the rainfall lasts later into the evening and nighttime.

Over each of the islands, there are low clouds between 2.5 and 2.8 km, but the cloudiness varies by temperature, shown in Figure 13 (F). The 301 K and 301.5 K SSTs have approximately 0.37 g/kg of cloud mixing ratios and the 303 K SST island has a cloud mixing ratio of 0.022 g/kg. As height increases, there are variations between the different temperatures and cloud coverage leading to a set of higher clouds between 11 and 12 km that is consistent between the SSTs. There is a stark gap in the high clouds between the 302.5 K and 303 K SST islands and the other islands.

The relative humidity shows that higher SSTs are overall drier than the lower SSTs with large variations between 1.4 and 12 km, shown in Figure 13 (A). It is consistent across all islands that the relative humidity increases until 1.5 km where it reaches approximately 80 to 85%, then it slowly decreases with height. The lower relative humidity in runs with higher SSTs are likely a result of the fact that, in general, the saturation water vapor mixing ratio increases much faster with temperature than the water vapor that is evaporated from the ocean.

The vertical velocity is variable between the different cases, shown in Figure 13 (E). All of the islands follow a pattern of a negative vertical velocity at the surface, then an increasing vertical velocity until 1 km. After 1 km, SSTs from 300.5 K to 303 K vertical velocity decreases, but the 300 K island continues to increase, reaching a maximum of 0.12 m/s at 4.25 km. The other SSTs decrease between 3 and 6 km. Then, farther up in the atmosphere between 8 and 10 km, all of the points except for the 300 K SST run have another spike in vertical velocity. It is clear that as SST increases, a pattern emerges. The presence of more water vapor in warmer runs will likely lead to the release of greater amounts of latent heat, which, in turn, will cause greater vertical velocities in cloud updrafts.

The mixing ratio of the 302.5 K and 303 K SST islands are farther apart than the other temperatures which can be seen in the cloud coverage over the islands as well (not shown).

3.4.2 Island Coast

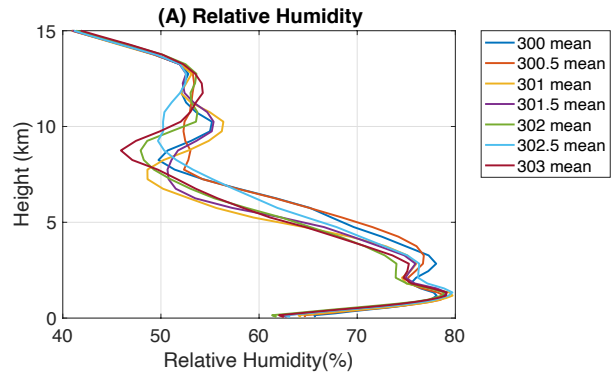

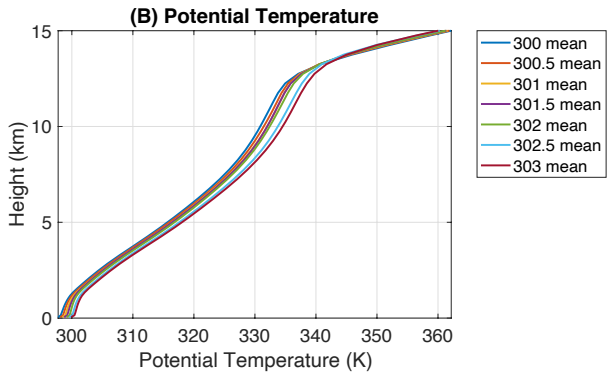

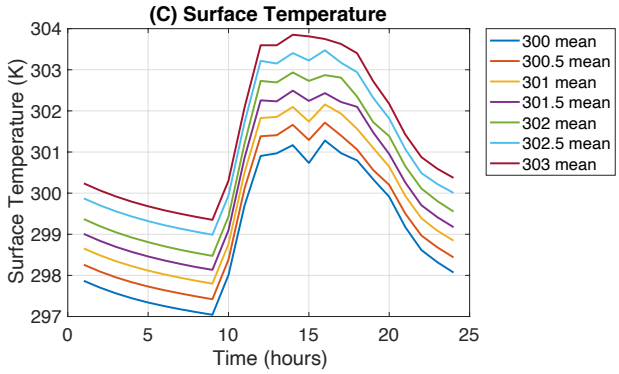

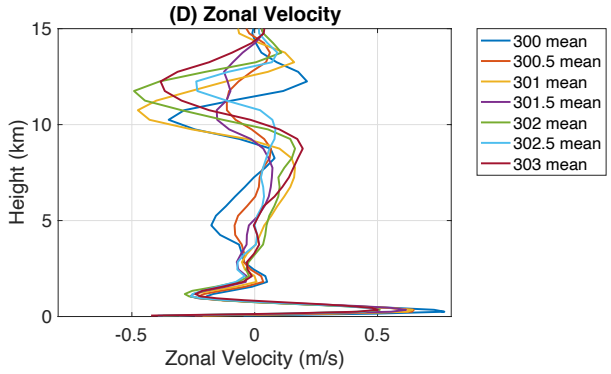

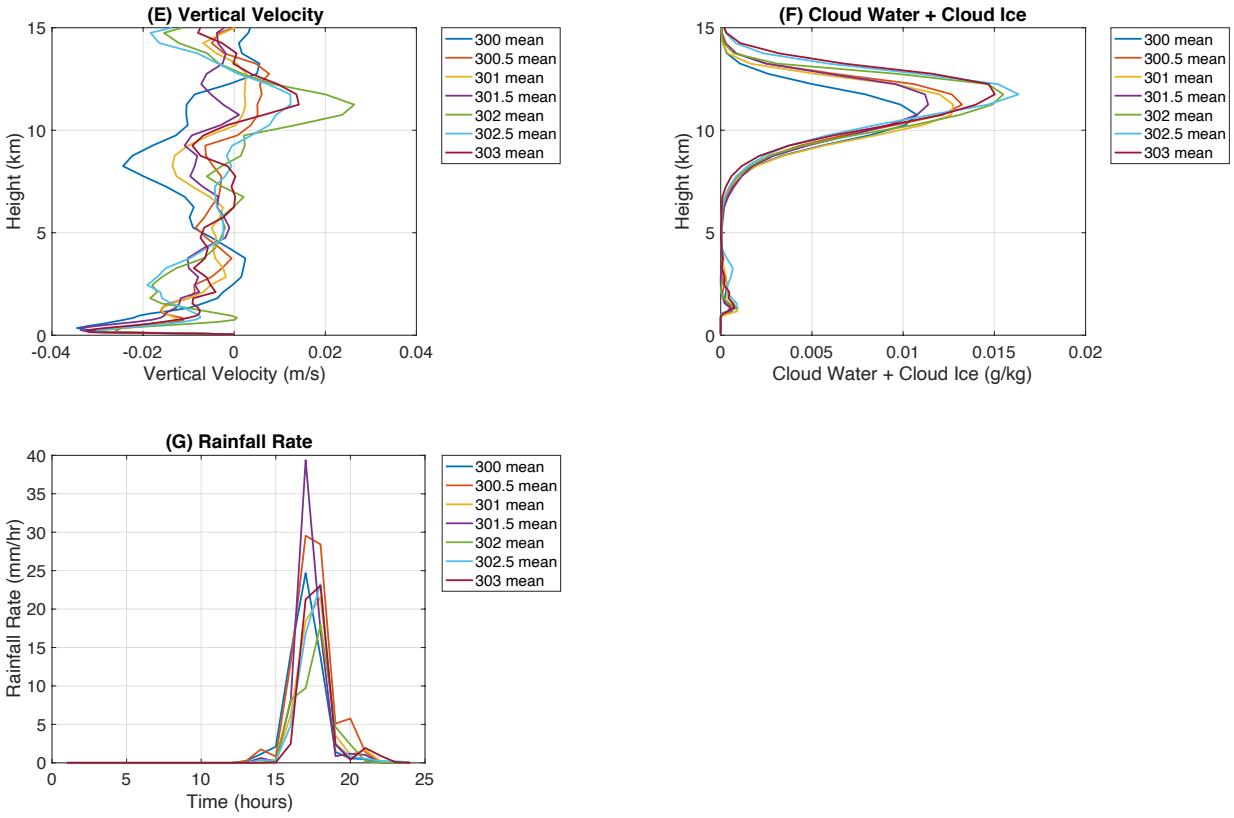

Figure 14: (A) The mean relative humidity for SSTs of 300K, 300.5K, 301K, 302.5K, 302K, and 303K on the average day on the coast of the flat, diurnal island in %. (B) The potential temperature for SSTs of 300K, 300.5K, 301K, 302.5K, 302K, and 303K on the average day on the coast of the flat, diurnal island in K. (C) The mean land surface temperature for SSTs of 300K, 300.5K, 301K, 302.5K, 302K, and 303K on the average day on the coast of the flat, diurnal island in K. (D) The mean zonal velocity for SSTs of 300K, 300.5K, 301K, 302.5K, 302K, and 303K on the average day on the coast of the flat, diurnal island in m/s. (E) The mean vertical velocity for SSTs of 300K, 300.5K, 301K, 302.5K, 302K, and 303K on the average day on the coast of the flat, diurnal island in m/s. (F) Mean cloud coverage for SSTs of 300K, 300.5K, 301K, 302.5K, 302K, and 303K on the average day on the coast of the flat, diurnal island in g/kg. (G) The mean rainfall rate for SSTs of 300K, 300.5K, 301K, 302.5K, 302K, and 303K on the average day on the coast of the flat, diurnal island in mm/hr.

On the coast of the islands, the variations of surface temperature look very similar throughout the various SSTs, shown in Figure 14 (C). At 9:00, surface temperature begins to rise, reaching a maximum at 14:00. At 15:00, starting at 300 K SST, there is a small dip in the surface temperature, then as the SST moves from 300.5 K to 303 K, the dip in temperature lessens. Following this, surface temperature begins to lower throughout the nighttime and early morning.

Potential temperature increases with height in all of the SSTs, but 302.5 and 303 K are a few degrees warmer than the other SSTs higher up in the atmosphere, shown in Figure 14 (B). Furthermore, 302.5 K and 303 K have a higher water vapor mixing ratio at the surface than the other SSTs (not shown). Generally, as the SST gets warmer, the relative humidity decreases on the surface, seen in Figure 14 (A). Higher up in the atmosphere, there are large variations in the relative humidity of about 5% between the SSTs, especially between 8 and 12 km. The 303 K island has the lowest relative humidity at 8 km of 46%. There is horizontal velocity at the surface of the 300 K coast of 0.77 m/s, and there is a clear pattern that as the SST increases from 300 K to 303 K, the horizontal velocity on the surface decreases which can be seen in Figure 14 (D). With variations in horizontal velocity with height, there is wind at 11 and 12 km in the 301 K and 302 K coasts of approximately 0.48 m/s.

There is the strongest negative vertical velocity on the 300 K coast of -0.035 m/s and as the SST warms from 300 K to 303 K, the negative vertical velocity decreases on the surface. Higher up in the atmosphere, at 8 km there is a negative vertical velocity in the 300 K coast, but a positive vertical velocity in the 302 K coast at 12 km, shown in Figure 14 (E). The 302 K coast is the only SST with significant positive vertical velocity.

Cloud patterns are similar on the coast of the various SST islands, shown in Figure 14 (F). There are very small low clouds, and higher up in the atmosphere around 11 to 12 km, there are far more high clouds. Overall, as the SST warms, there are more high clouds, the largest amount of high clouds over the 302.5 K coast. The 300 K coast has the lowest concentration of high clouds. This is likely a result of the larger amount of water vapor that is evaporated from warmer oceans.

Rainfall occurs at the same time of day at 17:00 in all of the SSTs, with small showers before and after larger rain which can be seen in Figure 14 (G). The 301.5 K coast has the largest rainfall rate of 39 mm/hr.

3.4.3 Ocean

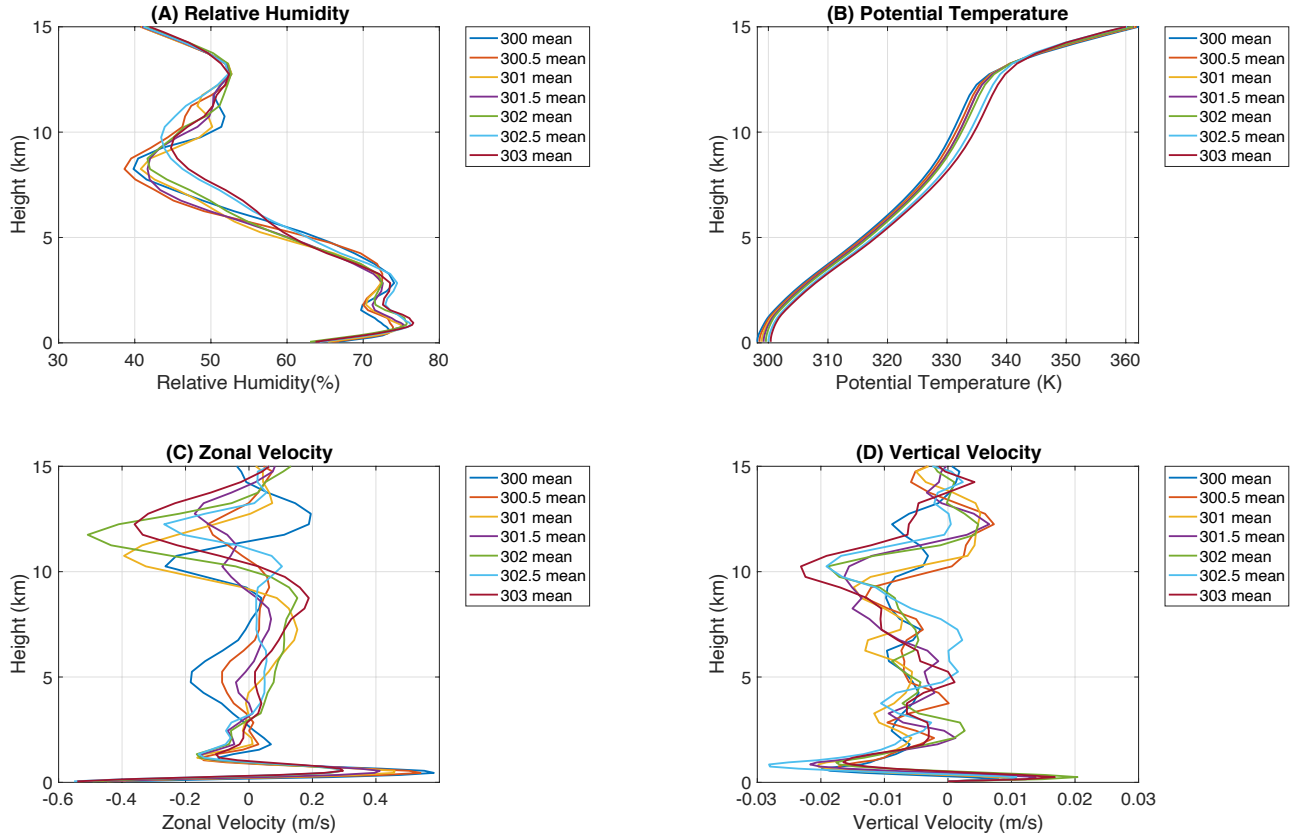

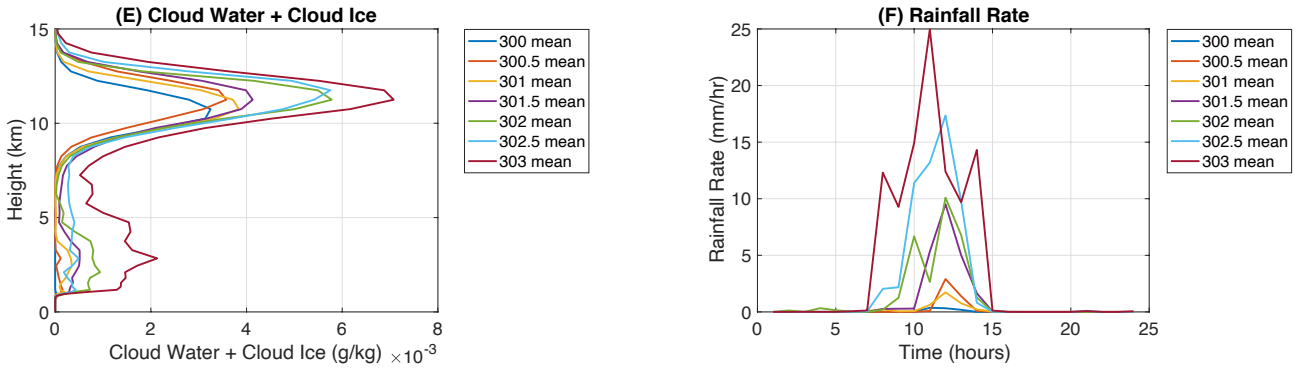

Figure 15: (A) The mean relative humidity for SSTs of 300K, 300.5K, 301K, 302.5K, 302K, and 303K on the average day over the ocean of the flat, diurnal island in %. (B) The potential temperature for SSTs of 300K, 300.5K, 301K, 302.5K, 302K, and 303K on the average day over the ocean of the flat, diurnal island in K. (C) The mean zonal velocity for SSTs of 300K, 300.5K, 301K, 302.5K, 302K, and 303K on the average day over the ocean of the flat, diurnal island in m/s. (D) The mean vertical velocity for SSTs of 300K, 300.5K, 301K, 302.5K, 302K, and 303K on the average day over the ocean of the flat, diurnal island in m/s. (E) Mean cloud coverage for SSTs of 300K, 300.5K, 301K, 302.5K, 302K, and 303K on the average day over the ocean of the flat, diurnal island in g/kg. (F) The mean rainfall rate for SSTs of 300K, 300.5K, 301K, 302.5K, 302K, and 303K on the average day over the ocean of the flat, diurnal island in mm/hr.

At 16 km above the ocean, surface temperature remains constant due to the infinite heat capacity of the ocean in the model. Because of this, the surface temperature of the ocean does not change in the diurnal cycle (not shown). The potential temperature is similar to the coast and middle of the flat island where 302.5 K and 303 K are slightly warmer than the other potential temperatures which can be seen in Figure 15 (B).

There is a pattern in relative humidity that as the SST warms from 300 K to 303 K, the relative humidity increases between 2 and 4 km and 7 to 9 km, generally decreasing with height. But over the ocean, as SST increases, the relative humidity rises slightly which is shown in Figure 15 (A).

There is negative velocity at the surface over the ocean, most prominent in the 302.5 K ocean, seen in Figure 15 (D). Moving higher up into the atmosphere, the vertical velocity is negative around 10 km in all of the SSTs.

Cloud mixing ratios are much smaller over the ocean than over the land or coast of the diurnal island as seen in Figure 15 (E). The higher clouds between 10 and 13 km

are much less concentrated, the largest being over the 303 K ocean. The lower clouds increase as SST increases, similar to the high clouds. The rainfall rate increases as SST increases over the ocean. There is almost no rainfall over the 300 K ocean and the greatest amount of precipitation over the 303 K island only reaches 25 mm/hr, shown in Figure 15 (F). As SST increases, rainfall occurs earlier in the day, but stops at the same time of 15:00. Rainfall over the 303 K island starts as early as 7:00 and continues until 15:00 and as SST increases, rainfall increases.

3.5 Mountainous Island with Diurnal Cycle Control

Following the modified flat island, we added a single bell-shaped mountain to the island of the same domain, seen in Figure 3.

3.5.1 Middle of the Island

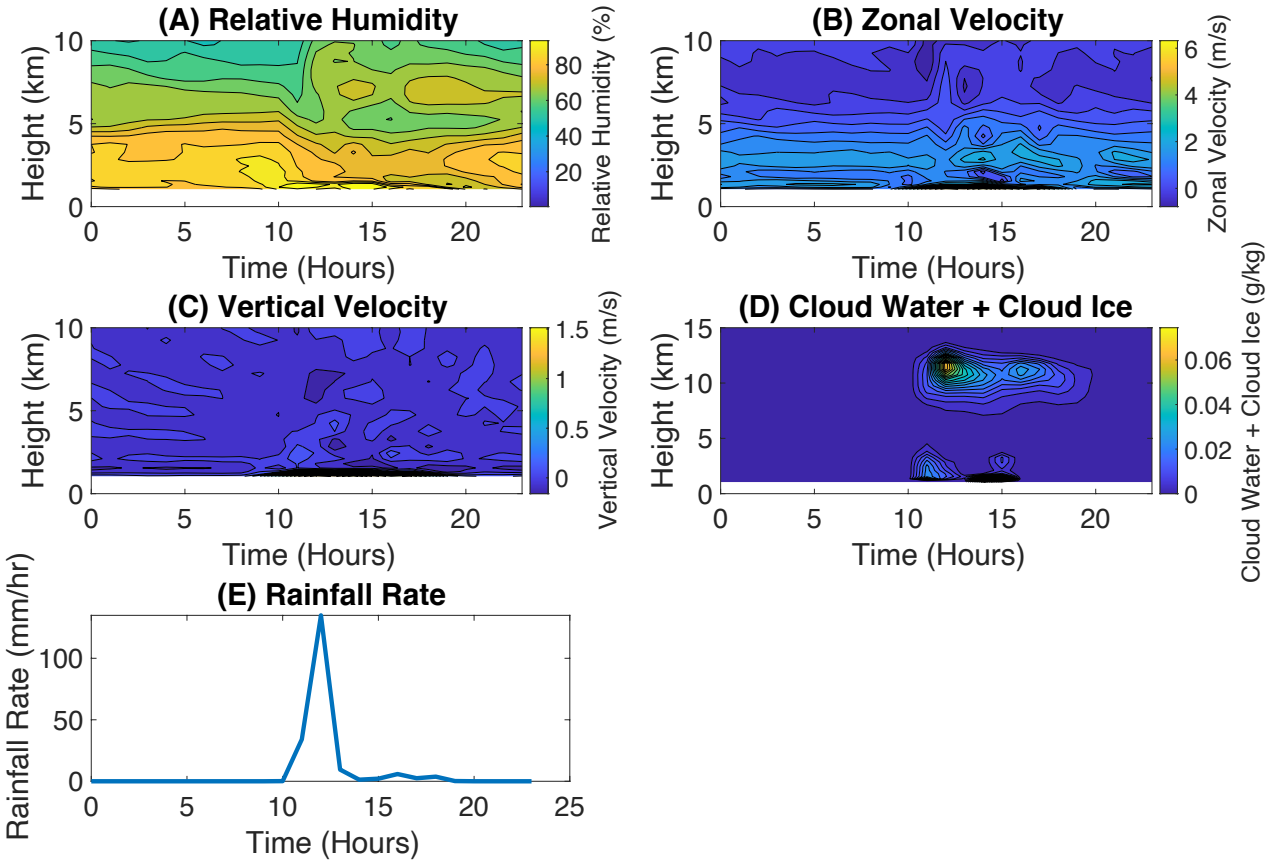

Figure 16: (A) Relative humidity throughout the average 300K day in the middle of the mountainous, diurnal island in %. (B) The zonal velocity throughout the average 300K day in the middle of the mountainous, diurnal island in m/s. (C) The vertical velocity throughout the average 300K day in the middle of the mountainous, diurnal island in m/s. (D) Cloud coverage throughout the average 300K day in the middle of the mountainous, diurnal island in g/kg. (E) Rainfall rate throughout the average 300K day in the middle of the mountainous, diurnal island in mm/hr.

The 300 K control island at 32 km is at the top of the mountain in the middle of the island. The surface temperature is coolest at 8:00 of 292 K. After 8:00, the temperature begins to rise throughout the day, but takes a slight dip at 12:00 shown in Figure 19 (C). The maximum temperature is reached at 14:00 of 308 K, then the temperature slowly drops throughout the evening and nighttime, reaching the lowest point again the next morning at 8:00.

There is no rainfall throughout the morning on the mountainous island until 11:00 which can be seen in Figure 16 (E). At 11:00 there is 130 mm/hr of rainfall which only lasts an hour, and then there is a much smaller peak of rainfall at 16:00 of less than 20 mm/hr which lasts for 3 hours until 19:00. Throughout the nighttime there is no rainfall.

There are very low clouds to the surface of the mountain between 1 and 4 km of 0.02 g/kg at 11:00 and a higher set of clouds from 7 to 13 km, shown in Figure 16 (D). The higher set of clouds lasts throughout the evening until 20:00, but the low set of clouds reaches even lower and touches the surface of the mountain from 13:00 to 16:00.

The relative humidity remains around 80% at the surface of the mountain until 11:00 and 14:00 where is increases to 95% which can be seen in Figure 16 (A).

There is minimal vertical velocity throughout the day, but between 10:00 and 15:00, there is a positive vertical velocity of 1.5 m/s very close to the surface of the mountain as seen in Figure 16 (C), possibly a manifestation of the updrafts that gives rise to the cloud and precipitation observed at that time. Furthermore, there is a positive horizontal velocity between 10:00 and 15:00 of 6 m/s that weakens throughout the evening, shown in Figure 16 (B).

3.5.2 Island Coast

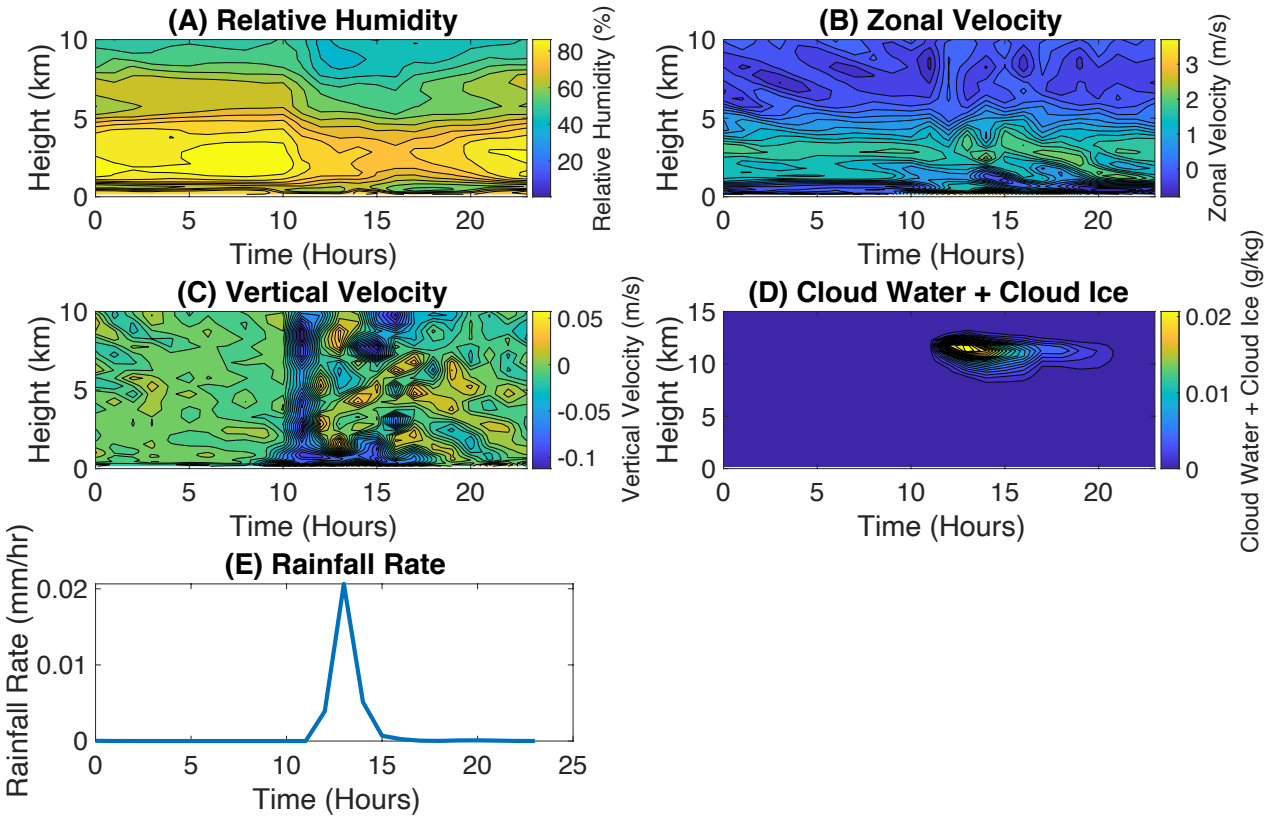

Figure 17: (A) Relative humidity throughout the average 300K day on the coast of the mountainous, diurnal island in %. (B) The zonal velocity throughout the average 300K day on the coast of the mountainous, diurnal island in m/s. (C) The vertical velocity throughout the average 300K day on the coast of the mountainous, diurnal island in m/s. (D) Cloud coverage throughout the average 300K day on the coast of the mountainous, diurnal island in g/kg. (E) Rainfall rate throughout the average 300K day on the coast of the mountainous, diurnal island in mm/hr.

On the coast of the 300 K mountainous island at 24 km, the surface temperature is lowest at 7:00 with a temperature of 298 K, shown in Figure 20 (C). Throughout the day, the temperature rises and reaches the maximum of 306 K at 14:00. Then, the temperature falls throughout the evening and nighttime until it reaches the low again at 7:00 the next morning.

There is minimal rainfall on the coast of the 300 K island compared to the middle of the island, seen in Figure 17 (E). At 13:00, there is a single peak in rainfall of 0.02 mm/hr, and then there is no more rain throughout the evening or night.

Clouds form at 11:00 between 8 and 12 km and last until 20:00, then there are no more clouds throughout the night or early morning which can be seen in Figure 17 (D).

Relative humidity remains close to 73% at the surface throughout the day, shown in Figure 17 (A).

Throughout the morning on the 300 K coast there is not much vertical velocity and then at 11:00, there is a negative vertical velocity of 0.1 m/s from the surface to 10 km, shown in Figure 17 (C). Following this at 15:00, there is more negative vertical velocity close to the surface and high in the atmosphere at 8 and 10 km. Zonal velocity is mostly negligible, but between 11:00 and 18:00, there is 3.0 to 3.5 m/s of horizontal velocity at the surface, seen in Figure 17 (B).

3.5.3 Ocean

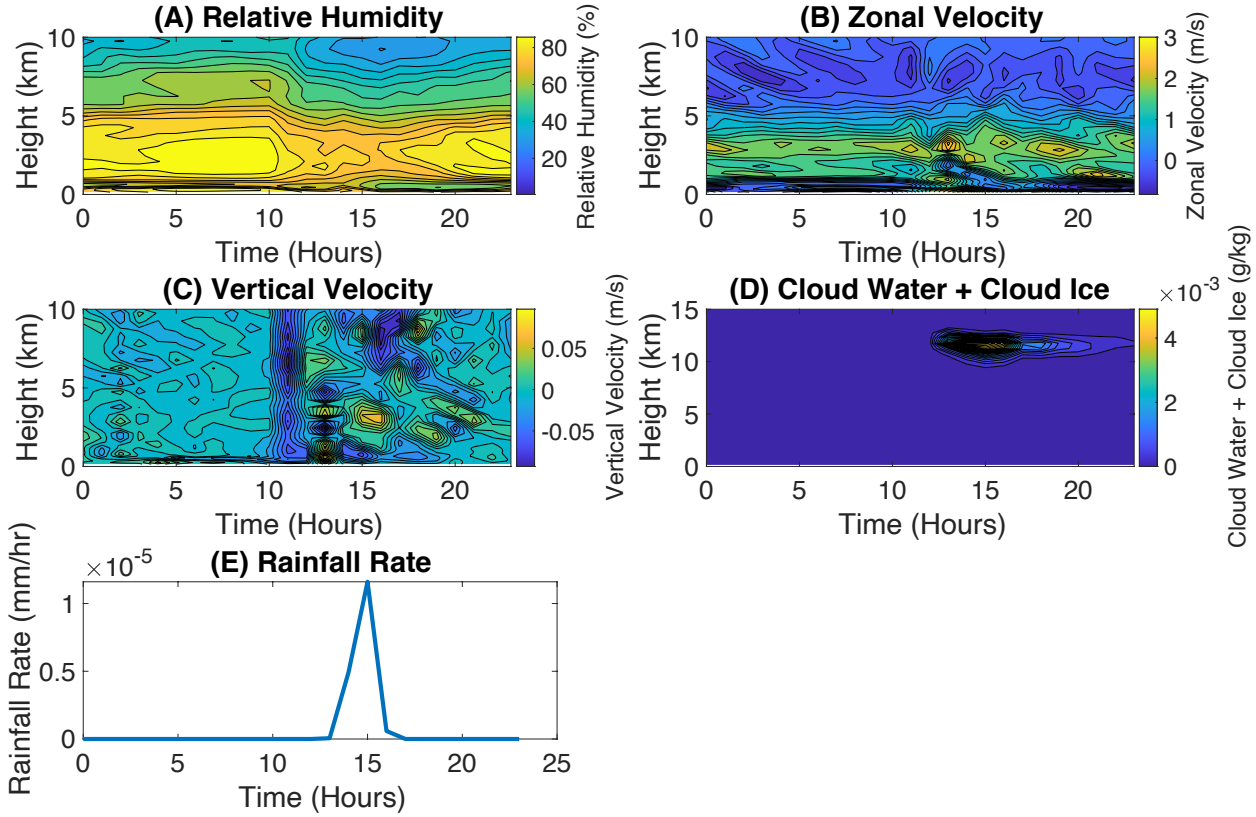

Figure 18: (A) Relative humidity throughout the average 300K day over the ocean of the mountainous, diurnal island in %. (B) The zonal velocity throughout the average 300K day over the ocean of the mountainous, diurnal island in m/s. (C) The vertical velocity throughout the average 300K day over the ocean of the mountainous, diurnal island in m/s. (D) Cloud coverage throughout the average 300K day over the ocean of the mountainous, diurnal island in g/kg. (E) Rainfall rate throughout the average 300K day over the ocean of the mountainous, diurnal island in mm/hr.

On the ocean of the mountainous 300 K control island, the SST is constant since there is no surface heating from land (not shown). There is no rainfall throughout the morning over the ocean, but at 15:00, there is very light rain of 1.2×10^{-5} mm/hr, seen in Figure 18 (E). There is no more rainfall throughout the evening or nighttime. This suggests that most of the rainfall that takes place in the domain is concentrated almost exclusively on the island.

Clouds appear at 13:00 at 12 km and last until 23:00 but there are not very many, shown in Figure 18 (D). The relative humidity on the surface of the ocean is betwee 75 and 83% from 4:00 until 13:00, but then it decreases as the day progresses which can be

seen in Figure 18 (A). There is negligible vertical velocity during the morning, but at 11:00, there is -0.06 m/s of vertical velocity and at 13:00 there is 0.05 m/s of vertical velocity, shown in Figure 18 (C). Throughout the evening and nighttime vertical velocity is negligible. At 14:00, there is potisive zonal velocity of 3 m/s at the surface of the ocean which can be seen in Figure 18 (C).

3.6 Climate Change Runs of the Mountainous Island with Diurnal Cycle

SSTs were averaged and plotted as a function of height and time to compare with the flat islands. There was a hardware failure when running the simulation for the mountainous island and the results for the 302K SST were corrupted. Considering the computational costs, the model was not re-run since there was a clear trend with the other 6 SSTs. Therefore, 302K was removed from the plots for the mountainous island.

3.6.1 Middle of the Island

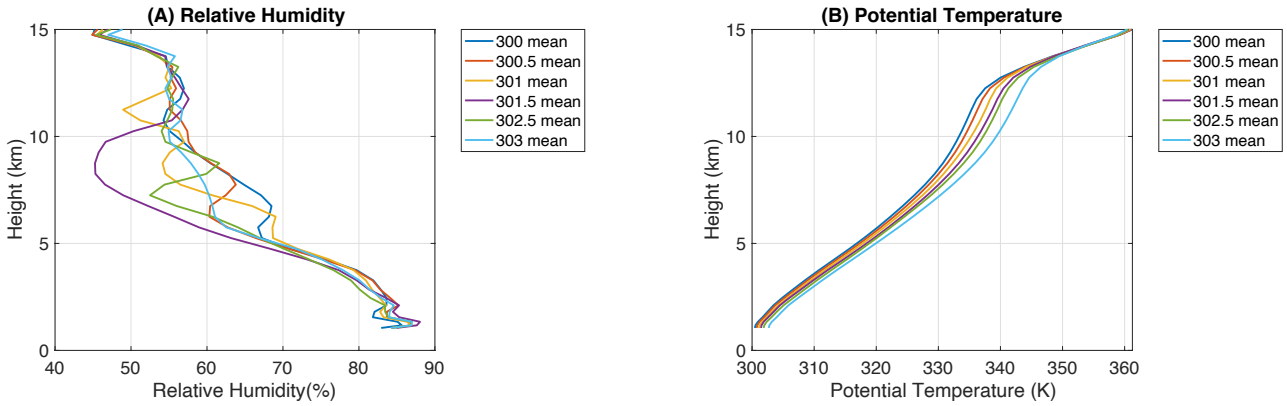

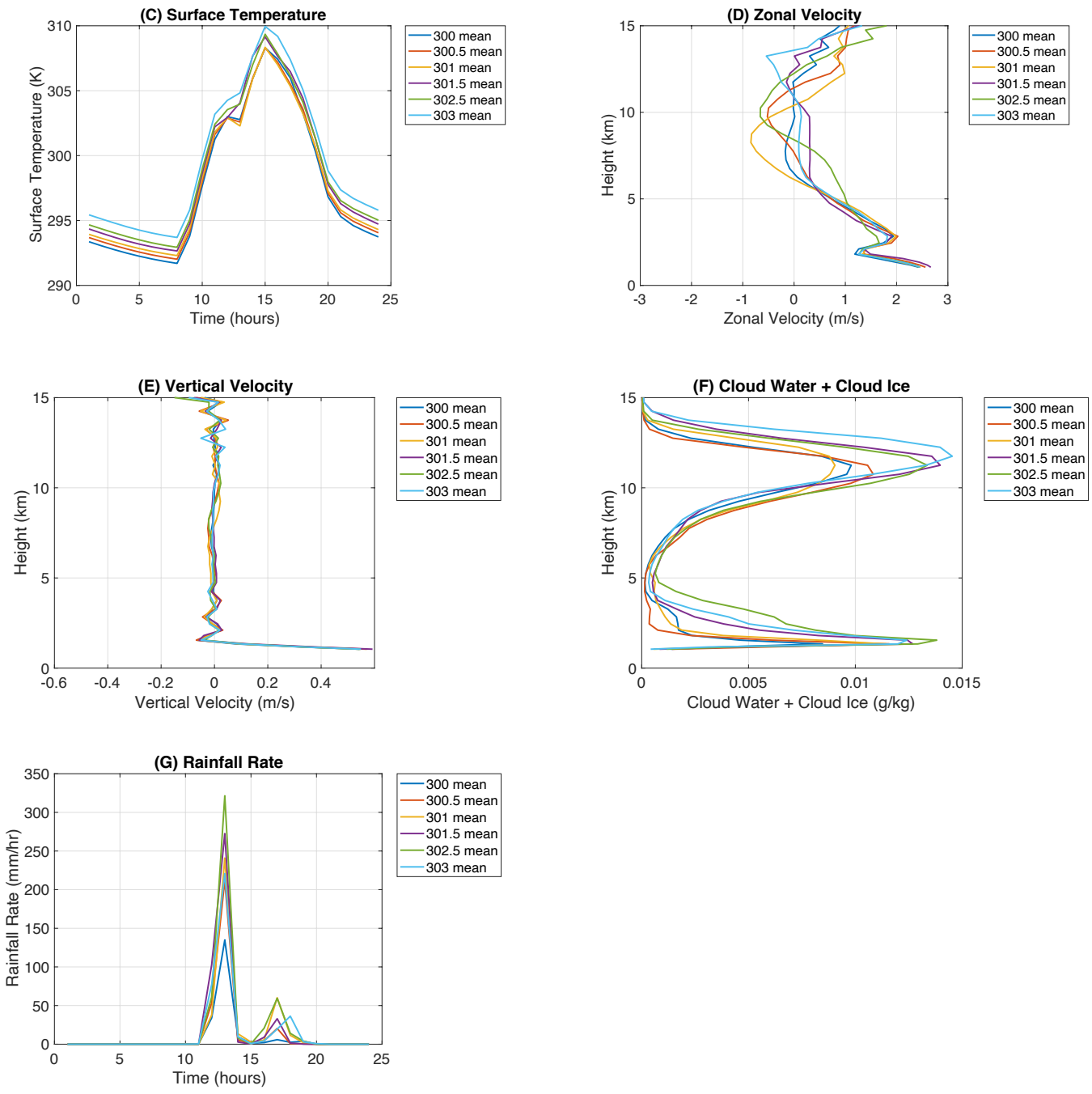

Figure 19: (A) The mean relative humidity for SSTs of 300K, 300.5K, 301K, 302.5K, 302K, and 303K on the average day in the middle of the mountainous, diurnal island in %. (B) The potential temperature for SSTs of 300K, 300.5K, 301K, 302.5K, 302K, and 303K on the average day in the middle of the mountainous, diurnal island in K. (C)The mean land surface temperature for SSTs of 300K, 300.5K, 301K, 302.5K, 302K, and 303K on the average day in the middle of the mountainous, diurnal island in K. (D) The mean zonal velocity for SSTs of 300K, 300.5K, 301K, 302.5K, 302K, and 303K on the average day in the middle of the mountainous, diurnal island in m/s. (E) The mean vertical velocity for SSTs of 300K, 300.5K, 301K, 302.5K, 302K, and 303K on the average day in the middle of the mountainous, diurnal island in m/s. (F) Mean cloud coverage for SSTs of 300K, 300.5K, 301K, 302.5K, 302K, and 303K on the average day in the middle of the mountainous, diurnal island in g/kg. (G) The mean rainfall rate for SSTs of 300K, 300.5K, 301K, 302.5K, 302K, and 303K on the average day in the middle of the mountainous, diurnal island in mm/hr.

In the middle of the mountainous island at 32 km, all of the islands reach their lowest surface temperatures at 8:00, shown in Figure 19 (C). They continue to rise throughout the morning, and they all take a slight dip around 13:00. This dip is likely due to evaporative cooling of rainfall. Because the middle of the island—which corresponds to the top of the mountain—seems to have clouds almost all the way down to the surface, rain doesn't have many chances to evaporate in a sub-saturated environment, which likely explains why the dip is smaller than what we observed in the flat island cases. The cooler SSTs take a larger dip than the warmer SSTs. All of the islands reach a maximum surface temperature at 15:00 between 308 and 310 K. SSTs of 300 K, 300.5 K, and 301 K all reach a maximum of 308 K. Then, the surface temperatures cool throughout the rest of the evening and nighttime.

Rainfall begins on all of the islands at 11:00 and in general, as SST increases, the rainfall rate increases as seen in Figure 19 (G). The island with 302.5 K SST has the highest amount of rainfall at 330 mm/hr and the 300 K SST has the lowest rainfall of 140 mm/hr. Rainfall stops by 15:00 and there is another small shower in all of the islands at 17:00. The higher the SST, the more rainfall in the second small shower. The island with 303 K SST has its secondary rainfall peak an hour later than the other islands at 18:00. Then rainfall stops throughout the evening and night. Rainfall rates change greatly as SST increases. There is a difference of 190 mm/hr between the 300 K and 303 K rainfall rate. Furthermore, the warmer SST runs begin raining quicker and last longer than the lower SST runs. There is a large delay in the secondary maxima of rainfall as SST increases, with the 303 K run lasting the latest into the evening.

In general, clouds appear at the same heights across SSTs, the amount of cloud mixing ratios just varies which can be seen in Figure 19 (F). There are low clouds at 1 km, and, as SST increases, the amount of cloud mixing ratios increases. The 300 K SST island has 0.009 g/kg of cloud mixing ratios and the 302.5 K SST island has 0.015 g/kg of cloud mixing ratios. Moving higher up, there is a second maximum of cloud mixing ratios at 10 and 11 km and in general, as SST increases, the amount of cloud mixing ratios increases. The 301 K SST island has 0.009 g/kg of cloud mixing ratios and the 303 K SST island has 0.014 g/kg of cloud mixing ratios.

On the surface, the relative humidity increases until 1 km and then begins decreasing until 13 km, shown in Figure 19 (A). The relative humidity is variable between SSTs between 5 and 10 km, but the island with 301.5 K SST has the minimum relative humidity of 45% at 8 km.

The vertical velocities are very similar between the various SSTs, starting with a positive vertical velocity of 0.7 m/s at the surface, seen in Figure 19 (E). Moving higher in the atmosphere, the vertical velocity remains around 0 m/s, with slight positive and negative changes. At 14 km, all of the islands have a negative vertical velocity between -0.35 m/s and -0.1 m/s. Zonal velocity is similar between SSTs close to the surface of the mountain with wind around 2.5 m/s, shown in Figure 19 (D). Increasing in height, the zonal velocity becomes variable between the SSTs. The mixing ratio of water vapor is similar between all of the SSTs, starting between 12 and 15 g/kg and decreasing with height (not shown).

3.6.2 Island Coast

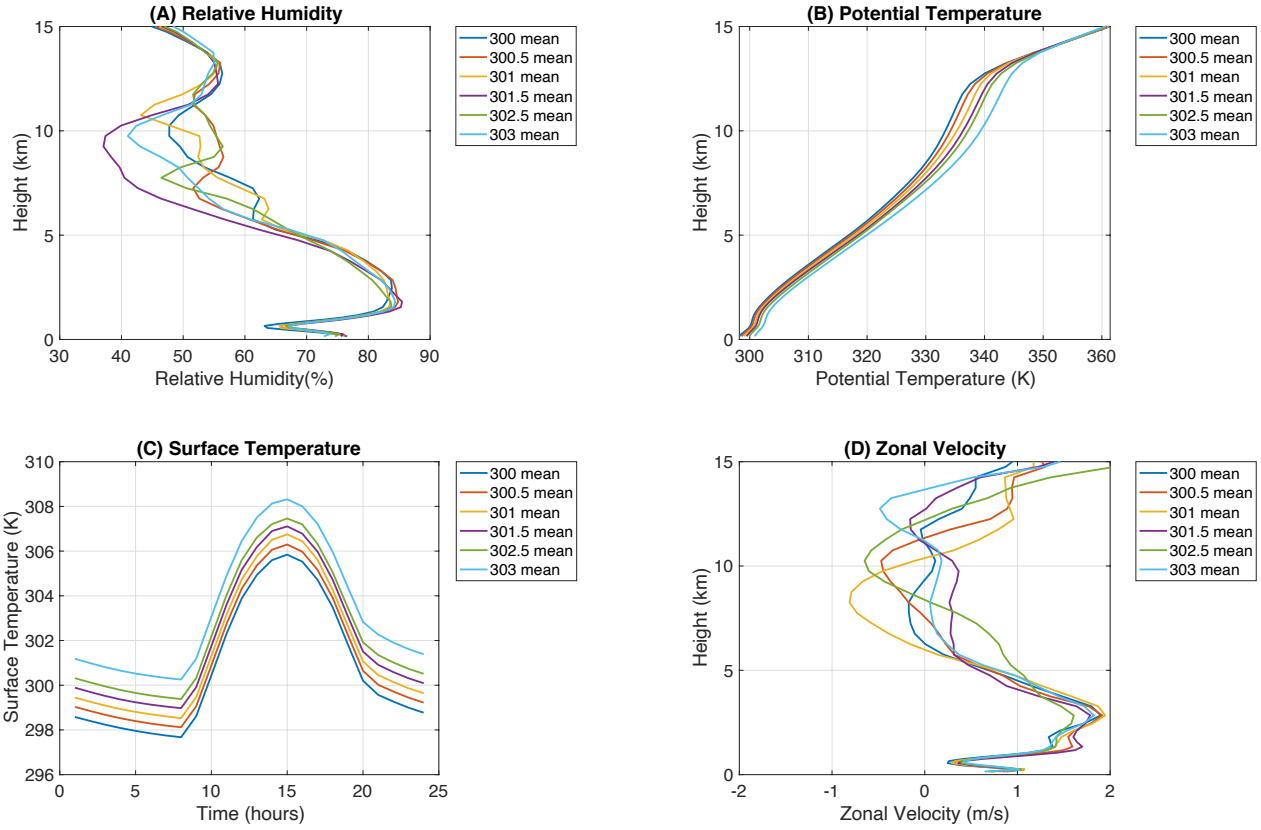

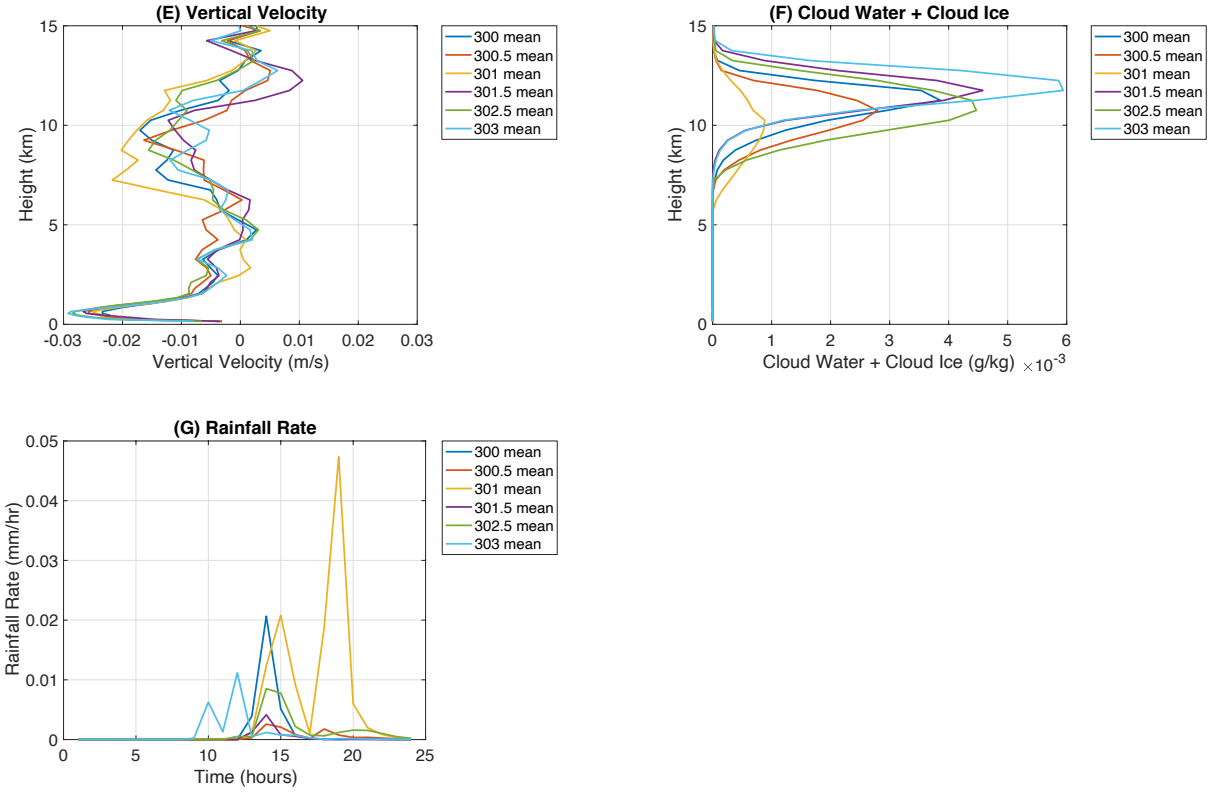

Figure 20: (A) The mean relative humidity for SSTs of 300K, 300.5K, 301K, 302.5K, 302K, and 303K on the average day on the coast of the mountainous, diurnal island in %. (B) The potential temperature for SSTs of 300K, 300.5K, 301K, 302.5K, 302K, and 303K on the average day on the coast of the mountainous, diurnal island in K. (C) The mean land surface temperature for SSTs of 300K, 300.5K, 301K, 302.5K, 302K, and 303K on the average day on the coast of the mountainous, diurnal island in K. (D) The mean zonal velocity for SSTs of 300K, 300.5K, 301K, 302.5K, 302K, and 303K on the average day on the coast of the mountainous, diurnal island in m/s. (E) The mean vertical velocity for SSTs of 300K, 300.5K, 301K, 302.5K, 302K, and 303K on the average day on the coast of the mountainous, diurnal island in m/s. (F) Mean cloud coverage for SSTs of 300K, 300.5K, 301K, 302.5K, 302K, and 303K on the average day on the coast of the mountainous, diurnal island in g/kg. (G) The mean rainfall rate for SSTs of 300K, 300.5K, 301K, 302.5K, 302K, and 303K on the average day on the coast of the mountainous, diurnal island in mm/hr.

On the coast of the mountainous island, the surface temperatures are lowest at 8:00 which can be seen in Figure 20 (C). They steadily increase until 15:00 where they reach the maximum surface temperatures between 306 K and 308 K. All of the surface temperatures follow a very similar pattern.

There is minimal rainfall on the coast of the island, and they peak at different times in the day, as seen in Figure 20 (G). In general, rainfall peaks between 10:00 and

15:00 with very low rates of 0.01 and 0.02 mm/hr. The maximum rainfall of 0.05 mm/hr is on the coast of the island with 301 K SST.

There are high clouds present between 10 and 12 km in all of the SSTs, but there are not very many clouds, shown in Figure 20 (F). These high clouds are possibly the result of detrainment from the deep clouds that develop over the mountainous island. In general, as SST increases, cloud concentration increases. The lowest cloud mixing ratio of $8x10^{-4}$ g/kg is present on the 301 K run coast and the highest cloud mixing ratio of $6x10^{-3}$ g/kg is present on the 303 K run coast.

The relative humidity is variable between the different SSTs but after decreasing at 1 km, the relative humidity reaches a maximum at 2 and 3 km of around 85%. Then, the relative humidity decreases with height with variations between 5 and 12 km. This can be seen in Figure 20 (A). The 301.5 K coast has the lowest relative humidity of 38% at 9 km.

The vertical velocity on the coast is more variable between SSTs than in the middle of the island, shown in Figure 20 (E). There is a negative vertical velocity between -0.03 and -0.024 m/s at 1 km that is similar between islands, but as height increases, there are larger variations between 3 and 12 km. The mixing ratio of water vapor is between 15 and 17 g/kg on the surface of the islands and as height increases, the mixing ratio of water vapor decreases (not shown).

3.6.3 Ocean

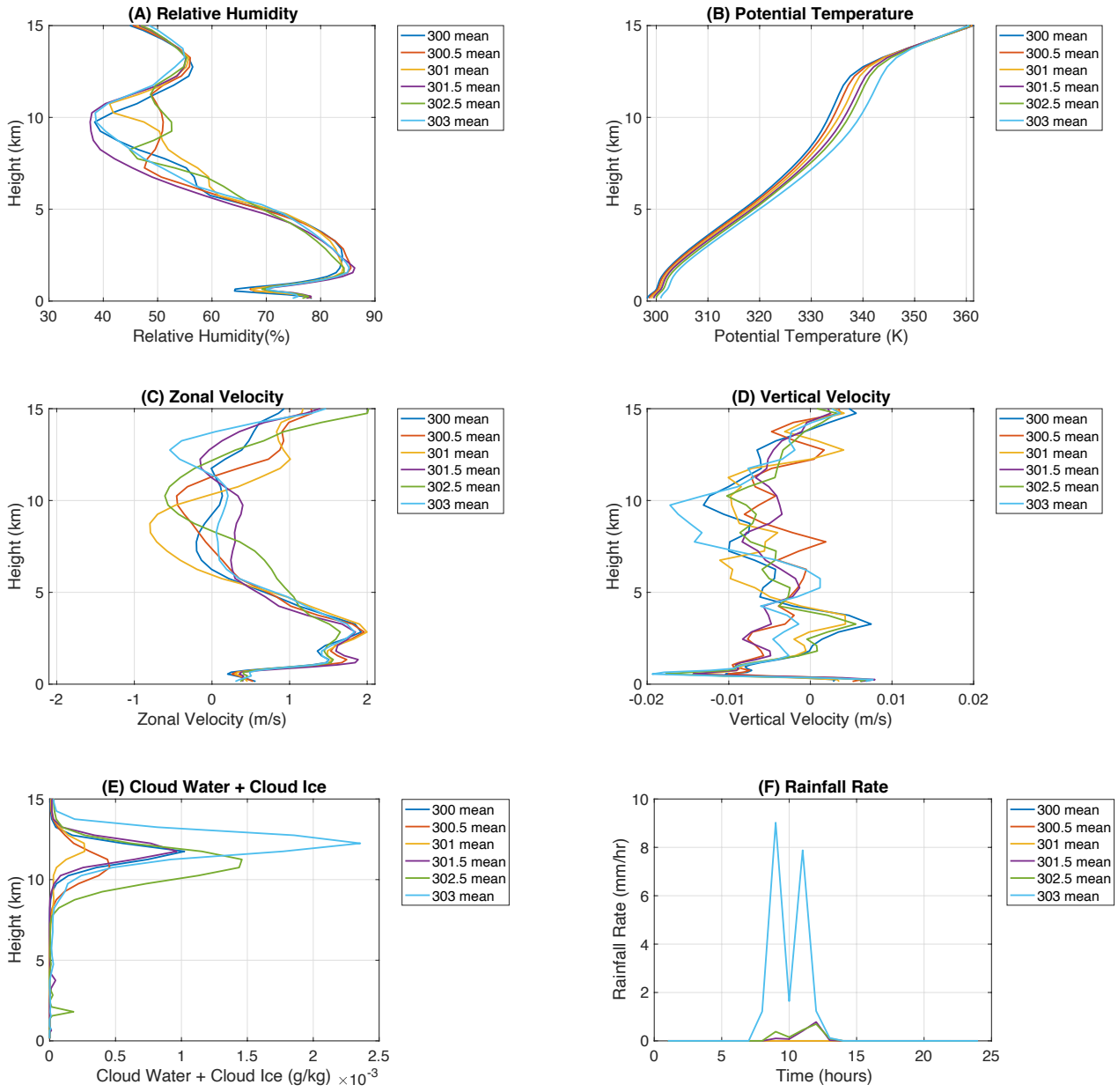

Figure 21: (A) The mean relative humidity for SSTs of 300K, 300.5K, 301K, 302.5K, 302K, and 303K on the average day over the ocean of the mountainous, diurnal island in %. (B) The potential temperature for SSTs of 300K, 300.5K, 301K, 302.5K, 302K, and 303K on the average day over the ocean of the mountainous, diurnal island in K. (C) The mean zonal velocity for SSTs of 300K, 300.5K, 301K, 302.5K, 302K, and 303K on the average day over the ocean of the mountainous, diurnal island in m/s. (D) The mean vertical velocity for SSTs of 300K, 300.5K, 301K, 302.5K, 302K, and 303K on the average day over the ocean of the mountainous, diurnal island in m/s. (E) Mean cloud coverage for SSTs of 300K, 300.5K, 301K, 302.5K, 302K, and 303K on the average day over the ocean of the mountainous, diurnal island in g/kg. (F) The mean rainfall rate for SSTs of 300K, 300.5K, 301K, 302.5K, 302K, and 303K on the average day over the ocean of the mountainous, diurnal island in mm/hr.

In the model, the ocean has an infinite heat capacity so the surface heating in the diurnal cycle does not affect the ocean surface temperatures (not shown).

Rainfall rate is minimal, but over the 303 K ocean, there is far more rainfall than the other SSTs, shown in Figure 21 (F). Rainfall peaks at various times, starting at 8:00 or 9:00 and going until 13:00 or 14:00. There are miminal low clouds over the ocean which can be sene in Figure 21 (E). Most of the clouds are located between 12 and 13 km and as SST increases, cloud concentration increases. The highest concentration of clouds are located above the 303 K ocean at $2.4x10^{-3}$ g/kg and the lowest concentration of clouds are located over the 301 K ocean at $3x10^{-4}$ g/kg. The relative humidity is around 75% at the surface and quickly decreases before reaching the maximum of around 84% at 3 km, seen in Figure 21 (A). This pattern is consistent in all of the SSTs and as height increases, the relative humidity decreases.

All of the SST runs reach a minimum around 10 km and the 301.5 K ocean has the lowest relative humidity of 38%. The vertical velocity is variable between runs at most heights, but it is consistent that there is a slight positive vertical velocity close to the surface of 0.007 m/s that quickly switches to negative vertical velocity of -0.02 m/s, seen in Figure 21 (D). Moving up in height, there are variations between positive and negative vertical velocities. There is not a strong horizontal velociy over any of the oceans. At around 2 and 3 km, there is a horizontal velocity close to 2 m/s, but as height increases, the horizontal velocity decreases which can be seen in Figure 21 (C).

4.0 DISCUSSION

Across all islands, rainfall is greater in the middle of the island than over the ocean. The coastal areas bear more complicated characteristics than over the open ocean and the middle of the island. In the flat and mountainous island with a diurnal cycle, there is a sea breeze convergence that leads to convective clouds and the detrainments stretch over the coast and ocean, seen in Figure 22. The ascent of air in the middle of the island and descent of air over the ocean in the vertical velocities supports this.

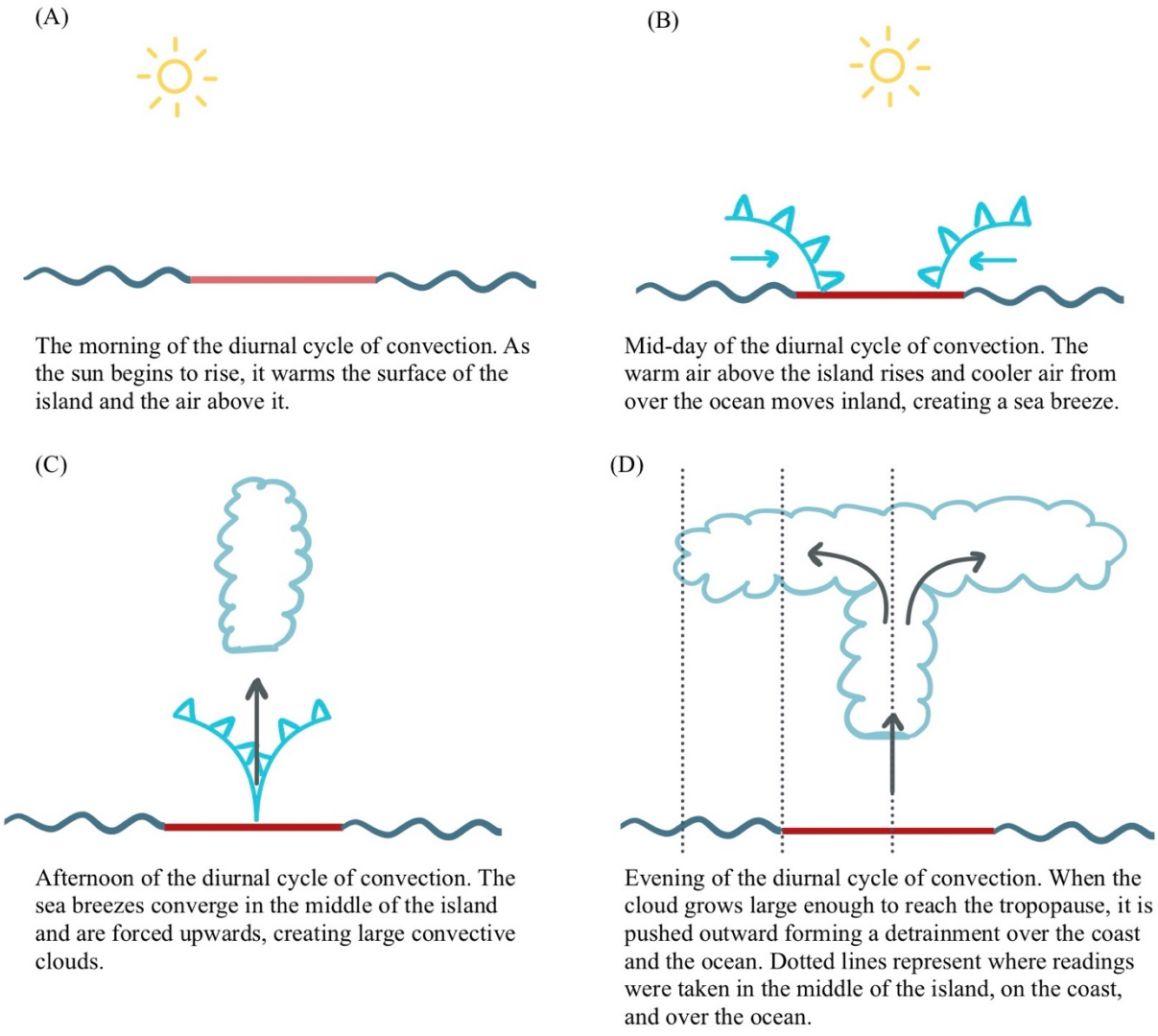

Figure 22: The diurnal cycle of convection on a flat island. (A) The morning of the diurnal cycle when the land is heated. (B) The middle of the day when the sea breezes move towards the middle of the island. (C) The afternoon when convective clouds start to form. (D) The evening, showing the outward motion of the clouds and the detrainments that form when reaching the troposphere.

4.1 Flat Island, No Diurnal Cycle

Rainfall rate is much greater over the middle of the island, then it lessens over the coast and is least apparent over the ocean. No diurnal cycle or background wind was imposed on these runs, which is why rainfall peaks at various times throughout the day depending on the SST. There is likely more rainfall over the middle of the island from the increased low-level cloud formations and there aren't as many clouds higher up in the troposphere. In the middle of the island, as SSTs got warmer, cloud formations lessened.

Moving from the middle of the island to the ocean, the air gets drier and the relative humidity lowers. The 302.5 K and 303 K mixing ratio of water vapor is slightly higher than the other SSTs and this could be due to larger heat fluxes over warmer oceans.

The vertical velocity is variable between the SSTs and at different parts of the island, but this is related to the cloud formations. The updraft accelerates when water vapor condenses and releases latent heat which makes the air parcel more buoyant. When the temperature of the island increases throughout the day, a pattern starts to emerge. Since this flat island has a fixed island temperature, diurnal cycles do not emerge.

This run was mostly intended as a preliminary check of the configurations of the model. The appearance of a strong zonal jet in the mid-tropospheric jet, while interesting to understand convection, makes it difficult to directly apply the results of this case to the real world.

4.2 Flat Island, with Diurnal Cycle

On the coast and in the middle of the flat diurnal island the cooler temperatures started raining earlier in the day and the warmer temperatures started raining an hour later which could be due to the potential of the clouds growing much larger and raining more with increasing temperatures. Furthermore, as SST increased, there are more clouds, supporting the hypothesis of them growing very large. Cloud peak is higher in the higher temperatures and at lower altitudes, there are more clouds with higher temperatures. Generally, higher SSTs are drier and the relative humidity decreases as SST increases, but over the ocean, as temperature rises, the air becomes more moist. The coast of the island is colder than the ocean for the majority of the day, so, since the surface of the land is much colder, this causes a net breeze shown as u, or the zonal velocity. During the nighttime, there is a strong land breeze, and during the day, there is a weaker sea breeze. This results in a strong net land breeze that is most prominent in the 300 K SST from surface heating.

In the middle of the island, there is a strong lifting of the air shown in the positive vertical velocity. This is possibly a result of the strong updrafts that develop as a result of the diurnal cycle of insulation like shown in Figure 22 (C). Over the ocean, subsidence appears to occur at 8 km altitude. This is the downward motion of an air parcel as it sinks in the atmosphere. This could be the descending branch of the circulation that develops over the island, further supporting the diurnal cycle of convection.

Towards the middle of the island, cloud mixing ratios are very large, almost 4 times as large as the cloud mixing ratios on the coast and ocean. In the middle of the island, there are more low clouds than on the coast and in the ocean which could be from

the developing convective clouds over the land. The disappearance of low clouds over the coast and ocean is likely due to the subsidence over the ocean confining the low clouds as the SST increases. The higher the SST over the middle of the island, the less low clouds due to their potential of growing very large.

Rain peaks over the middle of the island during the day and then on the coast in the afternoon. Typically, rain over the ocean peaks overnight due to the ocean and land contrast when there is no longer surface heating from the sun. In this case, the rain over the ocean takes place in the afternoon as well. This could be because higher up in the atmosphere, there is a detrainment from the large clouds in the middle of the island and the detrainment releases latent heat, stabilizing the atmosphere throughout the nighttime so the rain is delayed into the late morning, shown in Figure 22 (D). In the middle of the island, there is a delay of the secondary maxima of rainfall, but no delay in the initial peak. Furthermore, as SST increases, rainfall rate increases by almost 25% in the middle of the island. Warmer SSTs rain later in the day and have higher rainfall rates. This is likely due to the fact that the warmer SSTs take longer to build up, but once they do, they have more explosive qualities resulting in more rainfall and larger clouds.

4.3 Mountainous Island, with Diurnal Cycle

On the mountainous island, the surface temperature begins to rise earlier in the day than on the flat island. Rainfall rate is much greater in the middle of the island due to surface heating and sea breeze convergence which can be seen in Figure 22 (C), and rainfall begins at a consistent time no matter what the SST. Similar to the middle of the flat island, there is a secondary maximum in rainfall in the middle of the mountainous

island, but no delay in the initial rainfall as surface temperatures vary. The rainfall for the coast of the island is more variable and it rains in later parts of the day. Similarly, over the ocean, rainfall occurs during the morning or afternoon when rainfall over the ocean typically occurs during the nighttime. This is likely due to the detrainment from the clouds in the middle of the island releasing latent heat and stabilizing the atmosphere, shown in Figure 22 (D). When this happens, rainfall could be delayed through the nighttime to the late morning. But it is consistent throughout all areas of the island that as SST warms, rainfall rate increases. Cloud coverage is also greatest in the middle of the islands and moving towards the ocean, coverage decreases which can also be seen in Figure 22 (D). Consistently, as SST increases, cloud coverage increases due to its potential to grow much larger with warmer temperatures. Over the middle of the flat island, as SST increased, low cloud coverage decreased but the opposite is true over the mountainous island. There could be increased low clouds for the warmer SSTs due to the high positive vertical velocity from the diurnal cycle of convection and the sea breeze convergence in Figure 22 (B). Over the ocean, there is detrainment of condensate from the deep clouds over the middle of the island, so as SST increases, high cloud coverage increases shown in Figure 22 (D). Subsidence increases over the ocean which could be the descending branch of the island convection which would confine the low clouds as the SST increases. In the middle of the island there is a strong positive vertical velocity lifting the air, which then falls over the coast and ocean, supporting the ascent of air in the diurnal cycle. The air over the middle of the island has the highest relative humidity, but in general, the air above and around the mountainous island contains more water vapor than the flat diurnal island. This could be because the mountainous island has a

slightly larger surface area, resulting in more heating from the island which could create a warmer column above the mountain. The column above the mountain could then contain more water vapor which would cycle through the atmosphere and raise water vapor concentrations in other areas of the island.

5.0 CONCLUSION

In all of our simulations, the presence of a mountainous island enhanced the water vapor content in the atmosphere and the warmer SSTs resulted in higher rainfall rates and more clouds. Although more rain typically falls on mountainous islands than flat islands, in our study we found that the highest rainfall rates and cloud coverage come from the middle of the flat diurnal island because it has the strongest surface convergence (Dayem et al. 2007; As-syakur et al. 2013; Cronin et al. 2015). Warming the surface of the ocean increases the amount of water vapor over the oceans and above the islands which feeds larger clouds in the middle of the island, increasing the risk of heavy rain. Over the middle of the flat and mountainous island, there is an equal number of low clouds as there are high clouds whereas over the coast, low clouds begin to disappear. Our model results are consistent with other models from the Western coast of Sumatra which show that precipitation tends to peak in the early evening over land, but our results differ in that, over the ocean, precipitation occurs approximately at the same time or even earlier in the morning in some cases (Mori et al. 2004). This could be due to the detrainment from the middle of the island stabilizing the atmosphere, or it could also be a result of the relatively small domain sizes used in this study.

The enhancement of island rainfall could contribute to the localization of rising air over the Maritime Continent in relation to the Walker Circulation (Cronin et al. 2015). Our study suggests that islands favor large scale ascent while the surrounding oceans favor large scale subsidence, at least in the immediate vicinity to the island. This circulation could be affected by cloud or ocean feedbacks and the strength is difficult to estimate, but in our study, as SST increases, the strength of ascent over the middle of the

islands and subsidence over the ocean increases. The strength of this cycle and the rainfall that follows is very important to help future generations of islands in the tropics and the Maritime Continent with habitability and water security. As SST increases with climate change over mountainous islands, our models predict increasing rainfall and cloud coverage which cloud affect the daily weather and climate of certain islands in the tropics.

The results of our study were clear that in the middle of the diurnal islands, there is far more rainfall and clouds than the coast or ocean of the islands. Furthermore, as SST increased, rainfall rates and cloud mixing ratios increased in all areas of the islands, showing a stronger diurnal cycle. Over land of the mountainous and flat diurnal island, warmer SSTs caused a delay in the secondary peak of rainfall and for it to last longer into the evening and nighttime. In the middle of the islands, there are low and high clouds whereas when you move towards the ocean, low clouds dissipate. Over the oceans, although there is significantly less rain and clouds than over land, rainfall rates and cloud mixing ratios were much higher as SST increased compared to the lower SST runs.

This study shows that with anthropogenic climate change and warming ocean temperatures, there could be major changes in rainfall and cloud patterns in islands in the Maritime Continent including but not limited to, increased clouds and rainfall that last later into the nighttime. This study further explains why global changes in temperature might impact small islands more than large land masses and continents, although they are the smallest contributors to anthropogenic climate change (Lazrus 2012). Increased rainfall could increase the risk of water stress on the natural ecosystems of islands in the Maritime Continent which could affect native species and vegetation yield (Kang et al.

2019). Conditions similar to what was simulated in our model with low wind conditions or no wind, might appear in the doldrums near the Intertropical Convergence Zone (ITCZ) between the trade wind convergence. Furthermore, during El Niño and La Niña, there can be SST changes of 3 K similar to what we simulated, so increased rainfall and cloud coverage that lasts later in the day could appear in islands in the Maritime Continent during these years.

There were many limitations to our study, including, for example, the use of a simplified model. While idealized models are very useful to remove the interference from external, large-scale variability, the idealized nature of the simulations that we have created invites caution when applying the conclusions derived from this study to the real world. The relatively small area of the domain in which simulations are conducted is also another limitation, and sensitivity studies should be conducted to verify that our conclusions are not particularly sensitive to the domain size. Finally, in our study, we have only considered the effects of increasing sea surface temperatures, but climate change will likely manifest itself in many other ways, including changes over land. A detailed investigation of these effects will be the subject of future studies.

APPENDIX

Appendix 1

Table 1: Initial conditions for the flat, long channel, no diurnal island, the flat diurnal island, and the flat mountainous island.

Variables	Description of Variables	Flat Island No Diurnal Run/ Diurnal Run	Mountainous Island
nx	Total number of grid points in the x direction	512 / 128	128
ny	Total number of grid points in the y direction	3 / 128	128
nz	Total number of grid points in the z direction	62	62
nodex	Total number of processors in the x direction (For MPI runs)	16 / 8	8
nodey	Total number of processors in the y direction (For MPI runs)	1 / 8	8
terrain_flag	.true. = with terrain .false. = No terrain (flat lower boundary)	.false.	.true.
dx	Horizontal grid spacing in the x direction (m)	500.0	500.0
dy	Horizontal grid spacing in the y direction (m)	500.0	500.0
dz	Vertical grid spacing (m)	500.0	500.0
dtl	Large time step (s)	3	6
timax	Maximum integration time (s)	1728000.0	1728000.0
tapfrq	Frequency of three-dimensional model output (s)	3600.0	43200.0
rstfrq	Frequency to save model restart files (s)	86400.0	864000.0
statfrq	Frequency for calculating some interesting output (s)	3600.0	43200.0

cm1setup	0 = no subgrid turbulence model & no explicit diffusion 1 = large-eddy simulation (LES) 2 = mesoscale modeling with planetary boundary layer parameterization 3 = direct numerical simulation (DNS)	1	1
irst	Is this a restart? 0=no 1=yes	0/1	0/1
irdamp	Use upper-level Rayleigh damping zone? (acts on u, v, w, and theta) 0 = np 1 = yes, damp towards base state 2 = yes, damp towards horizontal average	1	1
wbc	Western boundary condition 1=periodic	1	1
ebc	East lateral boundary condition 1=periodic	1	1
sbc	South lateral boundary condition 1=periodic	1	1
nbc	North lateral boundary condition 1=periodic	1	1
bbc	Bottom boundary condition for winds where 1 = free slip 2 = no slip 3 = semi-slip	3	3
tbc	Top boundary condition for winds where 1 = free slip 2 = no slip	2	2
irbc	Type of radiative scheme to use: 4 = Durran-Klemp (1983) formulation	4	4
isnd	Base-state sounding 7 = External file named ‘input_sounding’ 11 = Saturated, constant equivalent potential temperature	11	11
iwnd	Base-state wind profile 0 = zero winds	0	0
itern	Initial topography specifications	0	1

	0 = no terrain 1 = bell shaped hill		
iinit	3D Initialization option 0 = no perturbations 1 = warm bubble	1	1
irandp	Include random potential temperature perturbations in the initial conditions? 0 = no 1 = yes	1	1
radopt	Use atmospheric radiation code? 0 = no 1 = yes, use the NASA-Goddard scheme The NASA-Goddard longwave and shortwave codes were adapted from the ARPS model, courtesy of the ARPS/CAPS group at the University of Oklahoma	1	1
dtrad	Time increment (s) between calculation of radiation tendency	300.0	300.0
ctrlat	Latitude (applies to entire domain, for now)	0	0
ctrlon	Longitude (applies to entire domain, for now)	-100	-100
isfcflx	Include surface fluxes of heat and moisture 0 = no 1 = yes	1	1
sfcmodel	Surface model (method to calculate surface fluxes and surface pressure) 1 = original CM1 formulation 2 = surface-layer scheme from WRF model Uses the MM5/WRF similarity theory code for the surface layer based on Monin-Obukhov with Carlson-Boland viscous sub-layer functions from look-up tables	1	2
oceanmodel	Model for ocean/water surfaces 1 = fixed sea-surface temperature 2 = ocean mixed layer model	1	1

initsfc	Initial surface conditions 1 = constant values (set tsk0, tmn0, xland0, lu0) 2 = sea breeze test case from WRF	2	2
tsk0	Default initial value for skin temperature (K) of soil/water 1 cm deep	300.0	300.0
tmn0	Default initial value for deep-layer temperature (K) of soil. Only used if sfcmodel = 2 and only used over land	297.0	297.0
lu0	Default initial value for land-use index (for water/ocean use 16)	16	16
season	which set of land-use conditions to use from file: 1 = summer values 2 = winter values	1	1
stretch_x	Use horizontally stretched grid in x? 0 = no	0	0
stretch_y	Use horizontally stretched grid in x? 0 = no	0	0
stretch_z	Use vertically stretched grid spacing? 0 = no 1 = Wilhelmson and Chen	1	1
ztop	Total depth of the domain (m)	25000.0	25000.0
str_bot	Level where stretching begins (m)	1000.0	1000.0
str_top	Level where stretching ends (m)	4000.0	4000.0
dz_bot	Grid spacing at (and below) str_bot (m)	100.0	100.0
dz_top	Grid spacing at (and above) str_top (m)	500.0	500.0
restart_format	Specifies the format of the restart files 1 = binary 2 = netcdf	1	1

Appendix 2

Table 2: Governing equations for calculated variables in Cloud Model 1 (CM1).

Variable	Variable Name	Governing Equations (Bryan 2017)
qv	Mixing Ratio of Water Vapor	$\frac{\delta qv}{\delta t} = ADV(qv) + T_{qv} + D_{qv} - \hat{q}_{cond} - \hat{q}_{dep}$
qc	Mixing Ratio of Cloud Liquid Water	$\frac{\delta qc}{\delta t} = ADV(qc) + T_{qc} + D_{qc} + \hat{q}_{cond} - \hat{q}_{frz} + \frac{1}{\rho}\frac{\delta(\rho V_c * qc)}{\delta z}$
qi	Mixing Ratio of Cloud Ice	$\frac{\delta qi}{\delta t} = ADV(qi) + T_{qi} + D_{qi} + \hat{q}_{dep} + \hat{q}_{frz} + \frac{1}{\rho}\frac{\delta(\rho V_i * qi)}{\delta z}$
u	Horizontal Velocity	$\frac{\delta u}{\delta t} + c_p\theta_p\frac{\delta \pi'}{\delta x} = ADV(u) + fv + T_u + D_u + N_u$
v	Meridional Velocity	$\frac{\delta v}{\delta t} + c_p\theta_p\frac{\delta \pi'}{\delta y} = ADV(v) + fu + T_v + D_v + N_v$
w	Vertical Velocity	$\frac{\delta w}{\delta t} + c_p\theta_p\frac{\delta \pi'}{\delta z} = ADV(w) + fw + T_w + D_w + N_w$
th	Potential Temperature	$\theta_p = \theta(\frac{1 + qv/\varepsilon}{1 + qv + ql + qi})$
prs	Pressure	
z	Height	
t	Time	
		$\hat{q}$ representing the phase change between the 3 components.

LITERATURE CITED

As-syakur, Abd Rahman, et al. “Indonesian Rainfall Variability Observation Using TRMM Multi-Satellite Data.” *International Journal of Remote Sensing*, 2013, doi:10.1080/01431161.2013.826837.

Bryan, George H. “The Governing Equations for CM1.” *National Center for Atmospheric Research*, 2017, pp. 1–15, http://www.mmm.ucar.edu/people/bryan/cm1/cm1_equations.pdf.

Coppin, David, and Gilles Bellon. “Physical Mechanisms Controlling the Offshore Propagation of Convection in the Tropics: 1. Flat Island.” *Journal of Advances in Modeling Earth Systems*, 2019, doi:10.1029/2019MS001793.

Cronin, Timothy W., et al. “Island Precipitation Enhancement and the Diurnal Cycle in Radiative-Convective Equilibrium.” *Quarterly Journal of the Royal Meteorological Society*, 2015, doi:10.1002/qj.2443.

Dayem, Katherine E., et al. “Tropical Western Pacific Warm Pool and Maritime Continent Precipitation Rates and Their Contrasting Relationships with the Walker Circulation.” *Journal of Geophysical Research Atmospheres*, 2007, doi:10.1029/2006JD007870.

Emanuel, Kerry A., and Raymond Hide. “ Atmospheric Convection.” *Physics Today*, 1995, doi:10.1063/1.2807986.

Fedorov, Alexey V., et al. “The Pliocene Paradox (Mechanisms for a Permanent El Niño).” *Science*, 2006, doi:10.1126/science.1122666.

Guichard, Françoise, and Fleur Couvreux. “A Short Review of Numerical Cloud-Resolving Models.” *Tellus, Series A: Dynamic Meteorology and Oceanography*, 2017, doi:10.1080/16000870.2017.1373578.

Hagos, Samson M., et al. “The Impact of the Diurnal Cycle on the Propagation of Madden-Julian Oscillation Convection across the Maritime Continent.” *Journal of Advances in Modeling Earth Systems*, 2016, doi:10.1002/2016MS000725.

Kang, Suchul, et al. “Future Climate Change Enhances Rainfall Seasonality in a Regional Model of Western Maritime Continent.” Climate Dynamics, vol. 52, no. 1–2, Springer Verlag, Jan. 2019, pp. 747–64, doi:10.1007/s00382-018-4164-9.

Lazrus, Heather. “Sea Change: Island Communities and Climate Change.” Annual Review of Anthropology, vol. 41, no. 1, Annual Reviews, 21 Oct. 2012, pp. 285–301, doi:10.1146/annurev-anthro-092611-145730.

Mori, Shuichi, et al. “Diurnal Land-Sea Rainfall Peak Migration over Sumatra Island, Indonesian Maritime Continent, Observed by TRMM Satellite and Intensive Rawinsonde Soundings.” *Monthly Weather Review*, 2004, doi:10.1175/1520-0493(2004)132<2021:DLRPMO>2.0.CO;2.

Neale, Richard, and Julia Slingo. “The Maritime Continent and Its Role in the Global Climate: A GCM Study.” *Journal of Climate*, 2003, doi:10.1175/1520-0442(2003)016<0834:TMCAIR>2.0.CO;2.

Peatman, Simon C., et al. “Propagation of the Madden-Julian Oscillation through the Maritime Continent and Scale Interaction with the Diurnal Cycle of Precipitation.” *Quarterly Journal of the Royal Meteorological Society*, 2014, doi:10.1002/qj.2161.

Qian, Jian Hua. “Why Precipitation Is Mostly Concentrated over Islands in the Maritime Continent.” *Journal of the Atmospheric Sciences*, 2008, doi:10.1175/2007JAS2422.1.

Raymond, David J., and Xiping Zeng. “Modelling Tropical Atmospheric Convection in the Context of the Weak Temperature Gradient Approximation.” *Quarterly Journal of the Royal Meteorological Society*, 2005, doi:10.1256/qj.03.97.

Robinson, Francis J., et al. “Resonant Response of Deep Convection to Surface Hot Spots.” *Journal of the Atmospheric Sciences*, 2008, doi:10.1175/2007JAS2398.1.

Ruppert, James H., and Xingchao Chen. “Island Rainfall Enhancement in the Maritime Continent.” *Geophysical Research Letters*, 2020, doi:10.1029/2019GL086545.

Schmidt, Helmut, and Ulrich Schumann. “Coherent Structure of the Convective Boundary Layer Derived from Large-Eddy Simulations.” *Journal of Fluid Mechanics*, 1989, doi:10.1017/S0022112089000753.

Sobel, Adam H., et al. “The Weak Temperature Gradient Approximation and Balanced Tropical Moisture Waves.” *Journal of the Atmospheric Sciences*, 2001, doi:10.1175/1520-0469(2001)058<3650:TWTGAA>2.0.CO;2.

Sobel, Adam H., et al. “Rain on Small Tropical Islands.” *Journal of Geophysical Research Atmospheres*, 2011, doi:10.1029/2010JD014695.

Wang, Shuguang, and Adam H. Sobel. “Factors Controlling Rain on Small Tropical Islands: Diurnal Cycle, Large-Scale Wind Speed, and Topography.” *Journal of the Atmospheric Sciences*, 2017, doi:10.1175/JAS-D-16-0344.1.

Yokoi, Satoru, et al. “Diurnal Cycle of Precipitation Observed in the Western Coastal Area of Sumatra Island: Offshore Preconditioning by Gravity Waves.” *Monthly Weather Review*, 2017, doi:10.1175/MWR-D-16-0468.1.